REVISITING METHYLOTROPHY: THE IMPACT OF LANTHANIDES AND LANTHANIDE-DEPENDENT ENZYMES ON THE METHYLOTROPHIC METABOLIC NETWORK

By

Anna Frances Huff

A THESIS

Submitted to
Michigan State University
in partial fulfillment of the requirements
for the degree of

Microbiology and Molecular Genetics – Master of Science

2017

ABSTRACT

REVISITING METHYLOTROPHY: THE IMPACT OF LANTHANIDES AND LANTHANIDE-DEPENDENT ENZYMES ON THE METHYLOTROPHIC METABOLIC NETWORK

By

Anna Frances Huff

The recent discovery of lanthanide (Ln^{3+})-dependent enzymes renewed interest in methylotrophs, although the impact of these enzymes is not understood. In *Methylobacterium extorquens* AM1, the Ca^{2+}-dependent MxaFI canonically oxidizes methanol to formaldehyde. The tetrahydromethanopterin (H_4MPT) pathway oxidizes formaldehyde to formate. Formate is oxidized to CO_2 by formate dehydrogenases (FDH) or partially reduced and assimilated. The genome of *M. extorquens* AM1 codes for three known Ln^{3+}-dependent genes: *xoxF*, *xoxF2*, and *exaF*. XoxF may oxidize both methanol and formaldehyde in some organisms while ExaF demonstrated efficient activity with formaldehyde in the presence of La^{3+} providing a potential alternative to the H_4MPT pathway.

RNAseq data provided by Dr. Nathan Good found downregulation of *mxa* genes and the first gene of the H_4MPT pathway, *fae*, and upregulation of *xoxF, xoxF2,* and *exaF* in the presence of La^{3+} suggesting changes to carbon distribution. I found a sharp decrease in accumulation formaldehyde and fourfold increase in accumulation of formate in the presence of La^{3+} and hypothesized this was due to the activity of Ln^{3+} enzymes. I measured the minimum inhibitory concentration (MIC) to methanol metabolism and found decreased sensitivity of a Δ*fae* mutant from 10 mM to more than 125 mM in the presence of La^{3+}. RNAseq suggested changes to the production of CO_2 which I corroborated finding an increased CO_2 production of 1.8-fold in the presence of La^{3+}. Together, these data provide the first profile of Ln^{3+}-dependent methylotrophic metabolism and provides new avenues for research.

ACKNOWLEDGEMENTS

I'd like to thank my advisor Dr. N. Cecilia Martinez-Gomez for her support and guidance throughout this project. Her support has been invaluable throughout my time at Michigan State University and has aided me in learning the skills necessary to complete this project. I'd also like to thank Dr. Nathan Good for his assistance with this project, particularly regarding the analysis of the RNAseq data, and for his always taking the time to answer my questions. Thanks particularly to Dr. Dan Jones, Dr. Scott Smith, Dr. Lijun Chen, Dr. Tony Schilmiller and the MSU Mass Spectrometry RTSF staff for their willingness to help me in all aspects of method development and data analysis for LC-MS/MS and GC-MS and their insight and guidance on method development and experimental design. Thanks to Dr. Rebecca Steidl and Dr. Gemma Reguera for the use of their gas chromatography equipment and teaching me how to use it. I'd like to thank Dr. Robert Hausinger and his lab for allowing me to use their lab equipment, borrow their tools, and occasionally supplying emergency experimental materials when mine ran out. I'd also like to thank my committee, Dr. Bob Hausinger and Dr. Michaela TerAvest, for supporting me and offering guidance whenever I needed it. I'd like to thank my lab mates, Dr. Paula Roszczenko and Olivia Walser, for cheering me up when I needed it and my friends and family for being very supportive.

TABLE OF CONTENTS

LIST OF TABLES

LIST OF FIGURES

KEY TO ABBREVIATIONS

Ln	Lanthanide
P_i	Inorganic phosphate
CBB	Calvin-Benson-Basham
EMC	Ethylmalonyl coenzyme A cycle
FBP	Fructose bisphosphate
Fdh	Formate dehydrogenase
H_4F	Tetrahydrofolate
H_4MPT	Tetrahydromethanopterin
KDPG	2-keto-3-deoxy-6-phosphogluconate
MDH	Methanol dehydrogenase
PQQ	Pyrroloquinoline quinone
DMS	Dimethyl Sulfoxide
Me-H_4F	Methelyne tetrahydrofolate
OD_{600}	Optical density at 600 nm
PES	Phenazine ethosulfate
MTBSTFA	*N*-Methyl-*N*-tert-butyldimethylsilyltrifluoroacetamide
CoA	Coenzyme A
PHB	Poly-β-hydroxybutyrate
MIC	Minimum inhibitory concentration

1: INTRODUCTION

Methylotrophic Metabolism

Methylotrophy is the ability of some microorganisms to use reduced compounds that lack carbon-carbon bonds as a sole source of both carbon and energy (1). This term can include the ability to use methanol, methane, methylated amines, halogenated methanes and methylated sulfur compounds (1). Methylotrophs live in diverse environments including both fresh and salt water, swamps and rice paddies, soil, and the plant phyllosphere (2–4). Methylotrophs can also be used for production of biofuels and bioplastics such as polyhydroxybutyrate (PHB).

Methylotrophy as a metabolic strategy was discovered in the early 20th century, and detailed studies of methylotrophic biochemistry began some 60 years ago (1, 5, 6). Methanol dehydrogenase (MDH) oxidizes methanol to formaldehyde (7). Methylamine is oxidized to formaldehyde using methylamine dehydrogenase or methylamine oxidase for Gram negative and Gram positive organisms respectively (8). Methylated sulfur species are converted first to dimethyl sulfate (DMS) which is in turn oxidized by the combined activity of DMS monooxygenase and a second oxygenase to produce formaldehyde and a sulfur product (8, 9). Methylotrophic bacteria may be broken into broad groups according to the biochemical strategy they rely on for carbon assimilation and energy production (2). Formaldehyde may be assimilated directly, as with type I methylotrophs, or it can be oxidized further to formate, as with type II methylotrophs, and a third group oxidizes it fully to CO_2 and uses the classical Calvin-Benson-Bassham (CBB) pathway for assimilation (1, 2). In this study, I will use the model organism *Methylobacterium extorquens* AM1, a facultative aerobic methylotroph able to use one, two, and four carbon compounds as growth substrates including methanol (10).

Type I methylotrophs rely on the ribulose monophosphate (RuMP) pathway in which formaldehyde is condensed with ribulose-5-phosphate to form glucose-6-phosphate or fructose-6-phosphate through the formation of hexose-6-phosphate (Figure 1) (1, 11). Fructose-6-phosphate is then cleaved leading to production of phosphoglycerate from pyruvate (1). Carbon balance using the RuMP pathway is as follows:

$$3 \text{ formaldehyde} + 1 \text{ NAD}^+ + 1 \text{ or } 2 \text{ ATP} \rightarrow \text{phosphoglycerate} + 1 \text{ NADH} + 1 \text{ ADP}$$

using the fructose-bisphosphate (FBP) aldolase variant or 2 ADP using the 2-keto-3-deoxy-6-phosphogluconate (KDPG) aldolase variant (1). Generally, obligate type I methylotrophs use the KDPG aldolase variant while facultative type I methylotrophs use the FBP aldolase variant (1).

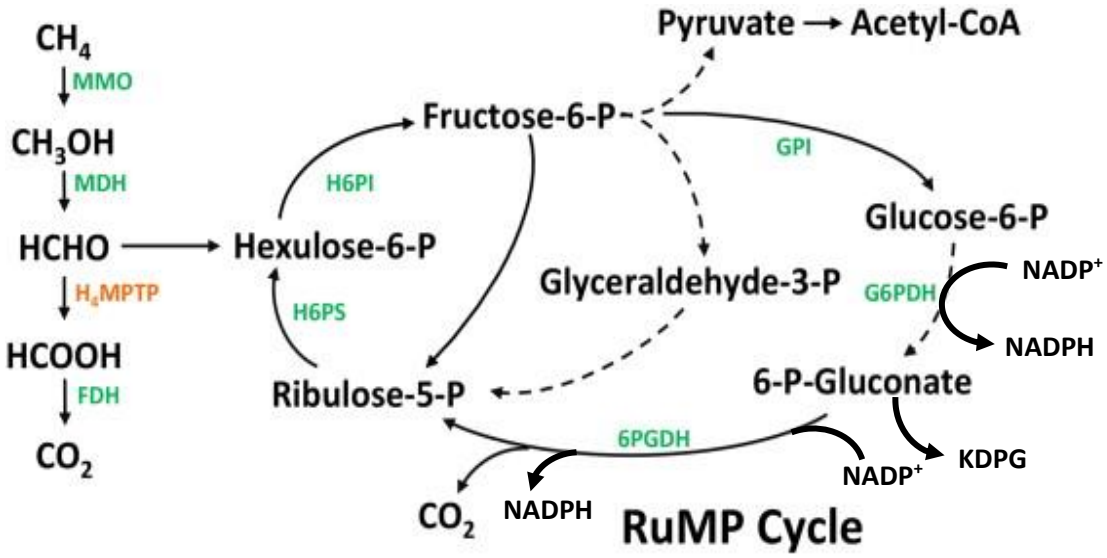

Figure 1 Simplified ribulose monophosphate pathway for type I methylotrophs using the KDPG aldolase variant. Dashed lines indicate possible pathways for production of biomass. Abbreviations are: MMO, methane monooxygenase, MDH, methanol dehydrogenase, H_4MPTP, tetrahydromethanopterin pathway, FDH, formate dehydrogenase, H6PI, hexulose-6-phosphate isomerase, GPI, glucose phosphate isomerase, G6PDH, glucose-6-phosphate dehydrogenase, 6PGDH, 6-phosphate-gluconate dehydrogenase, H6PS, hexulose-6-phosphate synthase. Reprinted with permission from Fei *et al.*, 2014.

M. extorquens AM1 is a Type II methylotroph, which relies on the serine cycle and EMC pathway for carbon assimilation (Figure 2) (1, 12). Instead of direct assimilation of formaldehyde, the tetrahydromethanopterin (H_4MPT) pathway oxidizes it to formate (11, 13, 14). Second, partial reduction of formate through the tetrahydrofolate pathway produces

methylene tetrahydrofolate (methylene-H_4F) (15, 16). Third, methylene-H_4F is condensed with glycine to form serine, the first intermediate in the serine pathway (1, 17). In most type II methylotrophs, including *M. extorquens* AM1, glyoxylate, the precursor of glycine, is regenerated by the EMC pathway since they lack the isocitrate lyase enzyme required for the glyoxylate shunt (18–20). A small minority of Type II methylotrophic genomes do encode functional genes for the glyoxylate shunt although they will not be discussed in detail here (1, 8). The overall carbon balance for type II methylotrophs are as follows:

$$3\ CH_2O + 5\ CO_2 + 6\ NAD(P)H + 2\ FAD + 5\ ATP \rightarrow 2\ C_4H_4O_5 + 2\ NAD(P)^+ + 2\ FADH_2 + 3\ ADP + 2\ AMP + 2\ PP_i + 3\ P_i \quad (12).$$

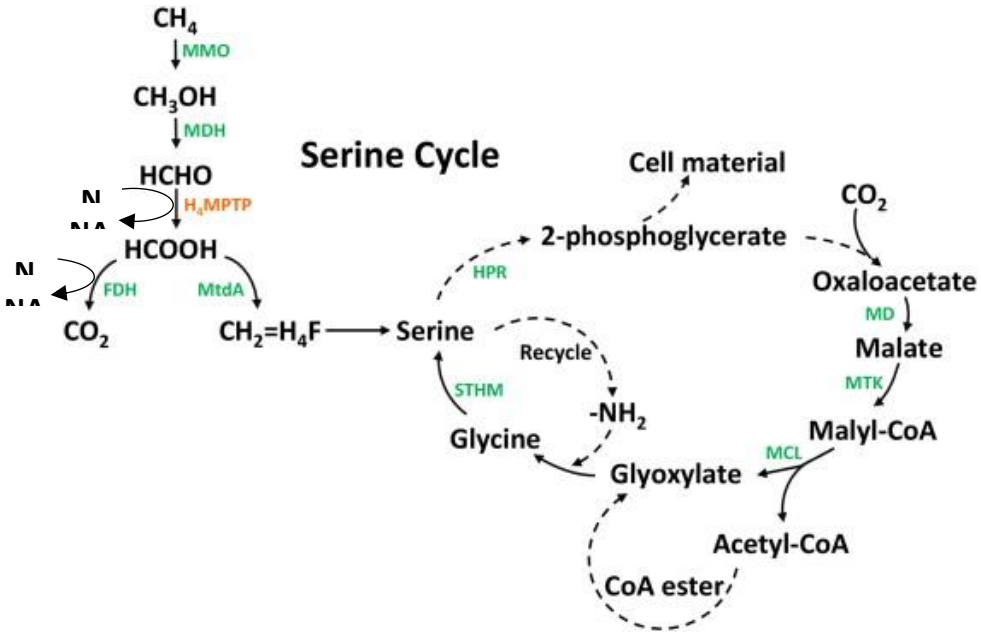

Figure 2 Simplified serine cycle for type II methylotrophs. Note that *M. extorquens* AM1 does not have a MMO and is therefore not able to oxidize methane. Dashed lines indicate possible pathways for production of biomass. Abbreviations are: MMO, methane monooxygenase, MDH, methanol dehydrogenase, H_4MPTP, tetrahydromethanopterin pathway, FDH, formate dehydrogenase, MtdA, methylene tetrahydromethanopterin dehydrogenase, HPR, hydroxypyruvate reductase, MD, malate dehydrogenase, MTK, malate thiokinase, MCL, malyl coenzymeA lyase, STHM, serine hydroxymethyl transferase. Reprinted with permission from Fei *et al.*, 2014.

The third type of methylotroph oxidizes formaldehyde to carbon dioxide before assimilation through the CBB pathway (Figure 3) (2). CO_2 and ribulose-1,5-bisphosphate are

used to make two molecules of the three-carbon compound 3-phosphoglycerate, which is converted to glyceraldehyde-3-phosphate. After one is isomerized, two molecules of glyceraldehyde-3-phosphate are then used to generate fructose-6-phosphate for use in biomass production (21). The overall carbon balance for methylotroph using the CBB pathway is as follows starting from CO_2:

$$6CO_2 + 18ATP + 12NADH(P)H + 12H^+ \rightarrow \text{fructose-6-phosphate} + 18ADP + 18\ P_i + 12NAD(P)^+$$

(21).

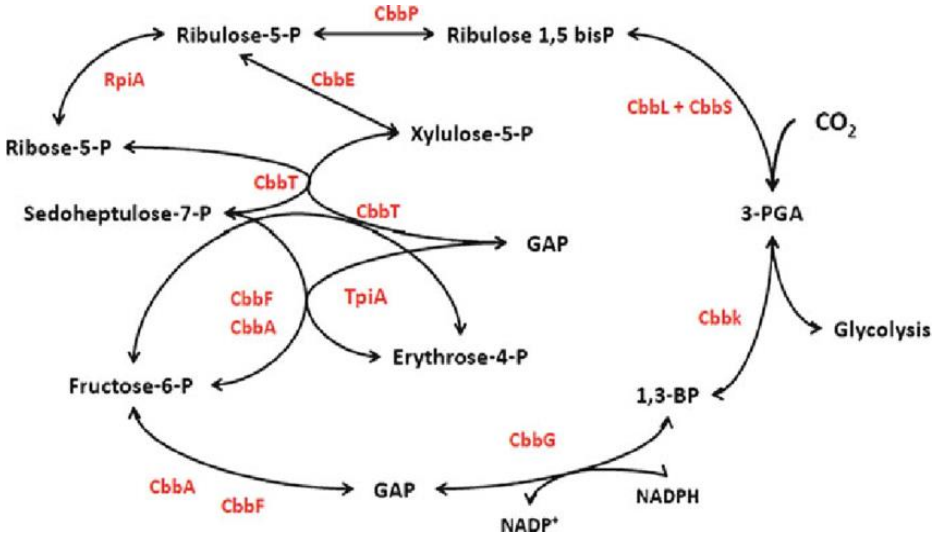

Figure 3 Schematic of the Calvin-Benson-Bassham cycle for CO_2 fixation in *Ralstonia eutropha*. Abbreviations are: Cbbk, phosphoglycerate kinase, CbbG, glyceraldehyde-3-phosphate dehydrogenase, CbbF, fructose bisphosphatase, CbbA, fructose-6-phosophate aldolase, TpiA, triosephosphate isomerase, CbbT, transketolase, RpiA, ribose-5-phosphate isomerase, CbbE, ribulose-5-phosphate epimersase, Cbbp, phosphoribulose kinase, CbbL+CbbS, ribulose-1,5-bisphosphate carboxylase/oxygenase (RuBisCO). Reprinted with permission from Brigham *et al.*, 2013.

Methanol Dehydrogenase

MDHs are a class of oxidoreductases found in both Gram-negative and Gram-positive bacteria (22). In Gram-negative bacteria, MDH is a periplasmic, pyrroloquinoline quinone (PQQ)-dependent, cytochrome-linked enzyme (22). In Gram-positive bacteria, MDH appears as a NAD(P)-linked cytoplasmic enzyme, although it's presence does not necessarily denote methylotrophic capability (23).

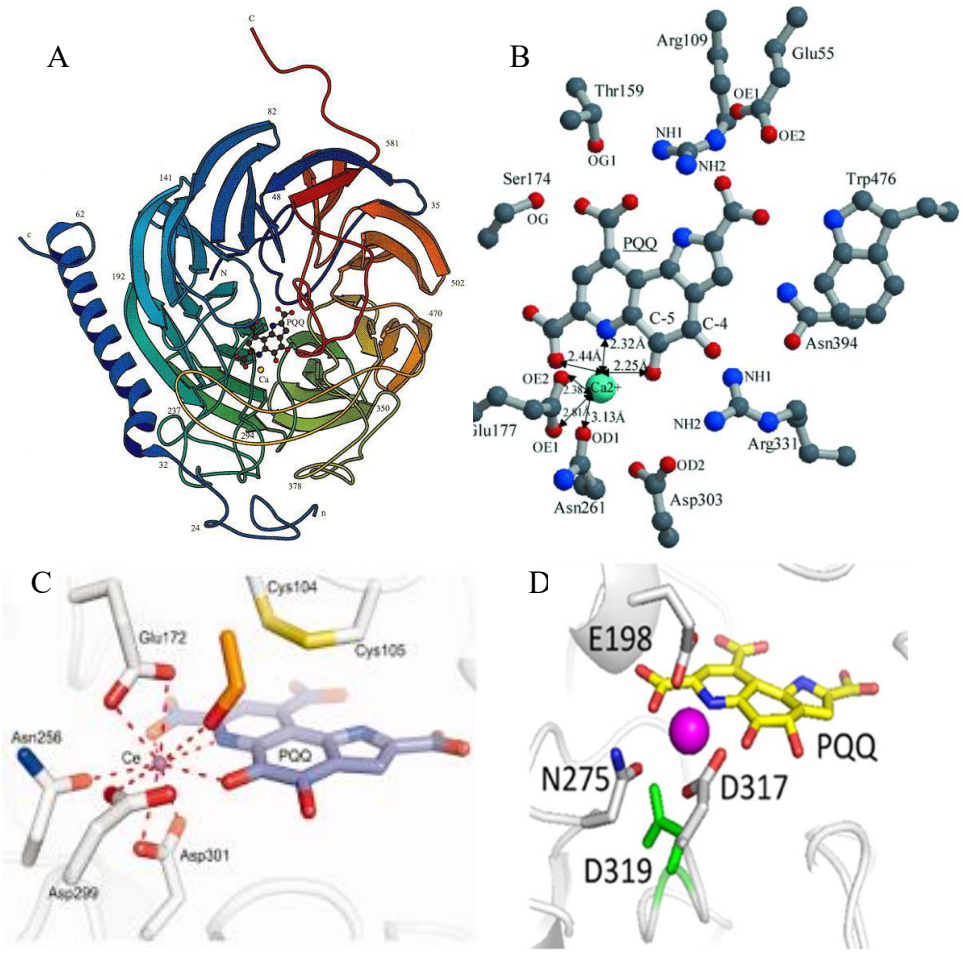

Figure 4 Structures of MxaFI from *M. extorquens* AM1 , XoxF from *M. fumariolicum* SolV, and ExaF from *M. extorquens* AM1. A) Crystal structure αβ of MxaFI from *M. extorquens* AM1. PQQ is shown in skeletal form with oxygen atoms in red. Ca^{2+} is shown in yellow. Reprinted with permission from Gosh *et al*, 1995. B) View showing coordination of PQQ and Ca^{2+} in the active sight of MxaFI from *M. extorquens* AM1. Reprinted with permission from Williams *et al*, 2005. C) View showing coordination of PQQ and cerium in XoxF from *M. fumariolicum* SolV. PQQ is show in blue. Cerium is shown in purple. Reprinted with permission from Pol *et al*., 2014. D) Homology model of ExaF active sight from *M. extorquens* AM1. PQQ is shown in yellow. La^{3+} is shown in magenta. Reprinted with permission from Good *et al.*, 2016.

PQQ is a non-covalently bound coenzyme found in some periplasmic dehydrogenases able oxidize substrates including methanol, ethanol, and glucose (Figure 4) (24). PQQ-dependent enzymes, in general, are diverse, presenting as monomeric or multimeric, soluble or membrane-bound, requiring only PQQ or additional coenzymes such as heme, and associated with many types of electron acceptors including cytochromes, ubiquinones, or blue copper proteins (24). PQQ-dependent MDHs are soluble, require only PQQ as a co-enzyme, and are linked to a C_L cytochrome electron acceptor (24). MDHs, such as the well-studied MxaFI, are heterotetrameric

with a $\alpha_2\beta_2$ structure (24). Each α subunit of MxaFI, encoded by the gene *mxaF*, contains one molecule of PQQ and one atom of a Lewis-acid (Figure 4) (24, 25). Until recently, it was believed that the Lewis acid of all MDHs was calcium (Ca^{2+}), but this has been challenged by findings that lanthanides (Ln) can be used by a different class of methanol dehydrogenases (24, 26–28). The β subunit of MxaFI, encoded by the gene *mxaI*, is very small at only 8.5 kDa and its function is not entirely clear (24).

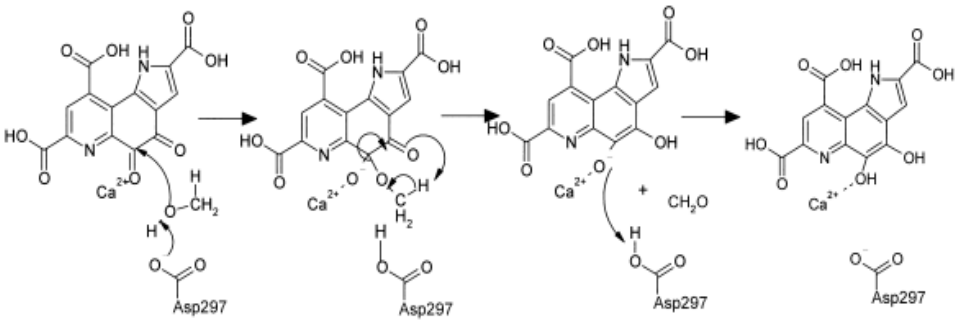

Figure 5 Mechanism of action for PQQ in methanol dehydrogenase. Oxidation of methanol initiates with proton abstraction by Asp297 followed by a nucleophilic attack at the 5C carbon of PQQ. The role of Ca^{2+} is proposed to be a Lewis acid acting to polarize the C=O bond by the alkoxide at the 5C position and stabilize intermediates during the proton abstraction and subsequent rearrangements. Reprinted with permission from Leopoldini *et al.*, 2007.

More recent research has focused on the role and catalytic properties of the XoxF MDH. XoxF shares 50% sequence identity with MxaFI and some properties including solubility, cellular location, and dependence on PQQ (29). However, a functional investigation into the catalytic properties of XoxF showed low activity using Ca^{2+} as a cofactor (29). In 2011 and 2012, two papers suggested that XoxF may be responsible for increased MDH activity in cell-free extracts after addition of La^{3+} and that XoxF expression increased in the presence of La^{3+} (30, 31). In 2014, the crystal structure of XoxF from a methylotroph found in a volcanic lake, *Methylacidiphilum fumariolicum* SolV, demonstrated the presence of Ce^{3+} in place of Ca^{2+} at the active site of the enzyme (Figure 4) (26). In this organism, XoxF was reported to have high catalytic efficiency with both methanol and formaldehyde (26). In contrast, the MxaFI enzyme

has relatively low efficiency with formaldehyde and this activity would, therefore, likely be physiologically irrelevant (22).

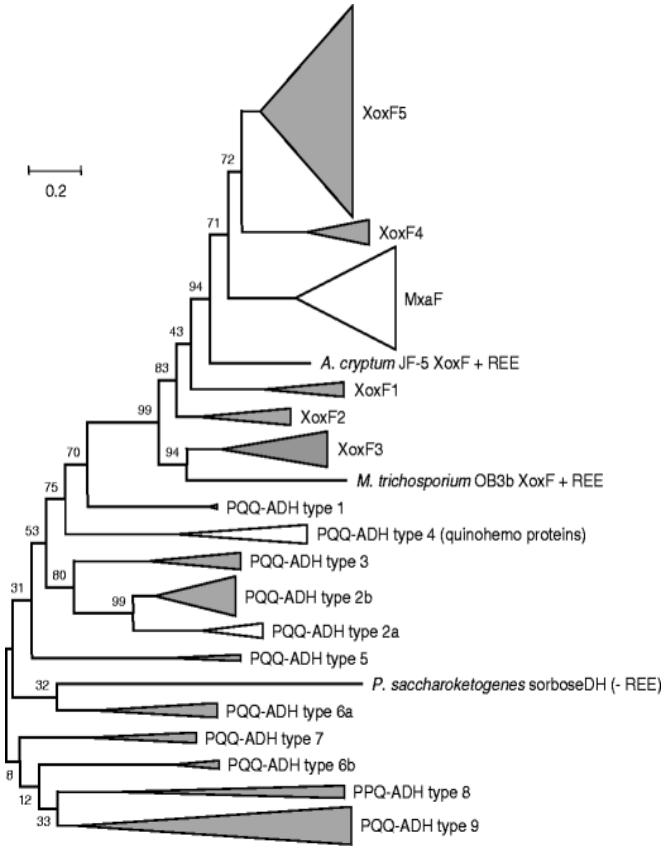

Figure 6 Phylogenetic tree of XoxF, MxaF and PQQ-dependent alcohol dehydrogenase proteins. Phylogenetic analysis of XoxF, MxaF, and alcohol dehydrogenase genes. XoxF from *M. extorquens* AM1 represents a XoxF5-type MDH. XoxF from *M. fumariolicum* SolV represents a XoxF2-type MDH.

Since the first report in 1996, the *xoxF* gene has been reported in a wide variety of methylotrophic communities (3, 32, 33). The *xoxF* gene has also been found in methylotrophs lacking the *mxaF* gene (3). Phylogenetic investigations have suggested that *xoxF* genes may predate *mxaF* genes and that Ca^{2+}-dependent enzymes evolved from those containing La^{3+} (Figure 6) (27). Further, the presence of Ln^{3+} in the XoxF enzyme, compared to the presence of Ca^{2+} in the MxaFI enzyme, has been proposed to allow for increased oxidation capacity, allowing for direct oxidation of HCHO in addition to CH_3OH (26, 27, 34).

In 2016, Exa, a novel and previously uncharacterized enzyme from *M. extorquens* AM1, demonstrated PQQ-dependent alcohol dehydrogenase activity in the presence of La^{3+} (28). Phenotypic studies had shown that an additional MDH was able to support methylotrophic growth in the absence of all known MDHs in the presence of La^{3+} and further biochemical and genetic analysis supported the role of ExaF as an MDH in methylotrophy (28, 35). Unlike MxaFI, ExaF showed high catalytic efficiency with formaldehyde suggesting a role for ExaF in the oxidation of formaldehyde during methylotrophic metabolism (28).

Rare Earth Elements and Lanthanide Chemistry

Contrary to their name, rare earth elements are not particularly rare (36). Their initial discovery in an unusual iron ore in 1798 gave rise to the misleading idea that rare earth elements were uncommon, although we now know these elements as a group to be more common than copper (36). Rare earth elements form insoluble minerals with phosphates, carbonates, silicates, and halides in deposits not concentrated enough to be economically beneficial for extraction which contributed to the misunderstanding of their abundance in the environment and misconception regarding their potential role in biological systems (36). In the last 100 years, rare earth elements have played diverse roles in the development of technology and influenced the course of modern life. From the early development of indoor gas lighting in the late 19^{th} century, which required cerium filaments, to modern applications in miniaturization of computers and production of permanent magnets, to negotiation of international trade deals necessary to secure materials for development of nuclear technology during the cold war, rare earth elements have played both a scientific and political role in shaping life in the 21^{st} century (36).

The Ln series of elements is a subset of rare earth elements: the 15 elements from lanthanum to lutetium. With the addition of yttrium and scandium, they are referred to as rare earth elements (37). From the base of La^{3+}, with the electron configuration $[Xe]5d^{1}6s^{2}$, the Ln series fills electrons in the 4f orbital (37). The geometry of f-orbitals compared with d- and s-orbitals means that 4f orbital electrons are likely to be found closer to the atomic nucleus than the 5d or 6s electrons leading to a phenomenon known as shielding where the 4f orbitals do not participate in forming bonds since they cannot penetrate the 5d and 6s orbitals (38, 39). This also leads to a phenomenon known as lanthanide contraction in which the atomic radii of Ln elements is larger than expected and does not decrease as sharply as with elements which lack f-orbital electrons (37, 40). Consequently, elements in the middle of the Ln series have a similar atomic radius to Ca^{2+} although their atomic number is much higher (37). In synthetic chemistry, this property has been uniquely useful because Ln, in general, share chemical properties with eachother as well as Ca^{2+} (41). The gradually decreasing atomic radius of the Ln series means that steric interactions of a complex can be reduced by choosing a Ln with optimal atomic radius whereas the sharply decreasing atomic radii in other elemental series means that chemically similar elements cannot easily substitute for each other within the same complex (41).

In general, Ln are found in the +3 state with Ln(III)/Ln(II) reduction potentials between -2.3V and -3.9V (41). Samarium, ytterbium, and europium are notable exceptions with reduction potentials of -1.55V, -1.15V and -0.35V respectively (41). The relatively low reduction potentials of Ln^{3+} are reflected in their oxidation capacity in complex with organic electron donors (42). Ln^{3+} series elements in general exhibit high oxidation potential in complex with organic electron donors (42). However, the high reduction potentials of samarium, ytterbium,

and europium mean they are relatively more stable in the Ln(II) state leading to decreased oxidation potentials in comparison with other Ln^{3+}-series elements (42).

Due to their similar size to Ca^{2+}, Ln^{3+} are also sometimes used as probes for studying Ca-binding proteins (43). In organic chemistry, the catalytic behavior of Ln^{3+} and Ca^{2+} are often compared because the limited radius of f-orbital electrons means that f-block elements, such as La^{3+} or Ce^{3+}, behave similarly to d-block elements (44). However, as Ln(III) is generally the most stable oxidation state for most Ln, the relatively lower charge density of Ca^{2+} means that Ln^{3+} may not easily substitute for calcium in catalytic roles despite similarities in ionic radius (45). Because Ca^{2+} and ytterbium are similar in ionic radius and, as previously mentioned, ytterbium is more stable than other Ln in a (II) state, it is more useful to compare the chemical behavior of these two elements rather than comparing Ca^{2+} to other Ln^{3+} ions (42, 44).

Modularity in Methylotrophy

Metabolism may be thought of as having modules that accomplish specific chemical goals (46). A module may be as simple as a single enzyme performing one task, such as methanol dehydrogenase, or as complex as an entire cycle with multiple enzymes, substrates and products, like the serine cycle (2). Modules can be separated from the metabolic network through several means including spatial means, such as being located in the periplasm instead of the cytoplasm, through high substrate specificity for the enzymes involved, or direct transfer of intermediates through multi-enzyme complexes (46). Modules may be regulated independently of a metabolic network to respond to specific environmental stimuli (47). This concept of modularity has been suggested to allow an organism to adapt to many environmental conditions easily and may be under strong, though indirect, evolutionary pressure since the modular nature

of metabolic networks allows for more robustness and reduces the impact of mutations on the network as a whole (48). In type II methylotrophs, and *M. extorquens* AM1 in particular, methylotrophic metabolism is traditionally broken down into four modules (Figure 7): oxidation of methanol to formaldehyde by MxaFI, oxidation of formaldehyde to formate by the tetrahydromethanopterin (H_4MPT) pathway, oxidation of formate to CO_2 by FDH, and assimilation of formate by the tetrahydrofolate, serine, and EMC pathways (2). With the recent characterization of XoxF and ExaF enzymes, we may add a potential fifth module: the Ln-dependent methanol/formaldehyde oxidation module (26, 28, 35).

The first module in methylotrophic metabolism is the oxidation of methanol to formaldehyde by the periplasmic MxaFI enzyme:

$$CH_3OH \rightarrow CH_2O + 2e^- + 2H^+ \quad (E_0' = -182\ mV) \text{ (27)}$$

MxaFI relies on the coenzyme PQQ and Ca^{2+} for activity (1). PQQ is a non-covalently bound coenzyme which acts as an electron acceptor during the oxidation of methanol (24). Ca^{2+} is thought to act to orient PQQ and methanol and polarize the C_5=O carbonyl bond (49). MxaFI activity is also linked to a dedicated C_L type cytochrome, MxaG, therefore generating ATP from methanol (1). MxaFI has been considered a hallmark of methylotrophy, and the *mxaFI* genes are often used to identify potential methylotrophs in the environment (50).

The second module of methylotrophic metabolism is the oxidation of formaldehyde to formate:

$$CH_2O + H_2O \rightarrow HCOO^- + 2e^- + 3H^+ \quad (E_0' = -534\ mV) \text{ (27)}$$

The H_4MPT pathway oxidizes formaldehyde in the cytoplasm using four enzymes: formaldehyde activating enzyme (Fae), methylene-H_4MPT dehydrogenase (MtdB), methenyl-H_4MPT cyclohydrolase (Mch), and formyl hydrolase/transferase complex (Fhc). The carbon carrier H_4MPT is an analog of tetrahydrofolate which can carry one-carbon compounds (13). Originally characterized in methanogenic and sulfur-reducing archaea, H_4MPT was later found in methylotrophic bacteria as well, and it was suggested that genes encoding H_4MPT-dependent enzymes were acquired through horizontal gene transfer from methanogenic archaea, potentially as a single transfer event (13). The pathway begins with Fae, or formaldehyde activating enzyme, which catalyzes the condensation of formaldehyde with H_4MPT to form methylene-H_4MPT and is essential for growth on methanol (13). Next, MtdB, or methylene-tetrahydromethanopterin dehydrogenase, catalyzes the dehydrogenation of methylene-H_4MPT to methenyl-H_4MPT, reducing one molecule of NAD(P) to NAD(P)H (E'_0*=-320 mV)* (51). Use of H_4MPT as opposed to H_4F is important in this step particularly as the reaction of methylene-H_4MPT to methenyl-H_4MPT, with a reduction potential of -390 mV, proceeds irreversibly whereas the analogous reaction with methylene-H_4F to methenyl-H_4F, with a reduction potential of -300 mV, is reversible (51). Mch, or methenyl-tetrahydromethanopterin cyclohydrolase, catalyzes the hydrolysis of methenyl-H_4MPT to formyl-H_4MPT (52). Fhc, or formyltransferase/hydrolase complex, catalyzes the hydrolysis of formyl-H_4MPT to formate and methanofuran via formation of formylmethanofuran (53). It has been suggested that hydrolysis of formate and H_4F involves a more negative free energy change than the hydrolysis of formate and H_4MPT helping to explain why condensation of formate and H_4F requires input of ATP whereas hydrolysis of H_4MPT and formate does not produce ATP (52).

The third module of methylotrophic metabolism is the oxidation of formate to CO_2 by FDH:

$$HCOO^- \rightarrow CO_2 + 2e^- \quad (E_0' = -430\ mV)\ (54)$$

In *M. extorquens* AM1, there are four known FDHs: Fdh1, Fdh2, Fdh3, and Fdh4 (55). Fdh1, Fdh2, and Fdh3 are tungsten or molybdenum-dependent enzymes and use iron-sulfur clusters for electron transfer (55, 56). Fdh1 and Fdh2 are also NAD-dependent while Fdh3 is cytochrome linked (56). Although little is known about Fdh4, previous work has demonstrated that deletion of *fdh4A* or *fdh4B* genes results in a toxic accumulation of formate and growth arrest (55). By contrast, deletion of any one or two of *fdh1*, *fdh2* or *fdh3* results in no detectable phenotype during growth on methanol (57). Deletion of all three of *fdh1*, *fdh2*, and *fdh3*, while not resulting in a change in growth rate, results in a transient accumulation of formate during lag phase and early exponential growth on methanol (57). While these results suggest that Fdh4 is the predominant FDH during growth on methanol, it also highlights the need to improve understanding of this enzyme since biochemical characterization and sequence analysis have previously failed to conclusively find a known electron acceptor for oxidation of formate by this enzyme (55).

The fourth module of methylotrophic metabolism includes a partial reduction of formate through the H_4F pathway beginning with condensation of formate and H_4F by the formate-tetrahydrofolate ligase enzyme FtfL and ending with the production of methylene-H_4F by the bifunctional methylene tetrahydromethanopterin dehydrogenase enzyme MtdA, an NADPH-dependent homolog of MtdB (15). Methylene-H_4F is incorporated into the serine cycle by the activity of the serine glyoxylate aminotransferase (Sga)/serine hydroxymethyltransferase (GlyA)

enzyme pair which each catalyze the transfer of an amino group: Sga transfers an amino group from serine to glyoxylate resulting in hydroxypyruvate and glycine while GlyA catalyzes the condensation glycine and methylene-H_4F to make serine (58). These enzymes are dependent on each other for activity since each provides a substrate for the other. The serine cycle produces three and four carbon compounds important for biomass production including 2-phosphoglycerate, oxaloacetate, and phosphoenolpyruvate (58). Glyoxylate is regenerated through the ethylmalonyl-CoA (EMC) pathway (58). The serine cycle and EMC pathway are resource intensive processes requiring three NADPH, two NADH, two ATP and three CO_2 per cycle (58).

I propose the inclusion of a fifth Ln-dependent module, which oxidizes methanol and formaldehyde to formate by Ln-dependent MDHs independently of the H_4MPT-pathway. Both XoxF from *Methyloacidiphilum fumariolicum* SolV and ExaF from *M. extorquens* have been shown to oxidize formaldehyde to formate with high efficiency [1, 5]. Interestingly, the Δ*mxaF xoxF1 xoxF2* mutant, while able to grow on methanol, exhibited a decreased growth rate only 30% of that found in the wild-type strain (28). This suggests that the primary role of ExaF *in vivo* is not oxidation of methanol. Biochemical data suggest the primary role of ExaF *in vivo* may be oxidation of formaldehyde (28).

The goal of my thesis project is to define the impact of the Ln-dependent module on the metabolic network of *M. extorquens* AM1 during methylotrophic growth and determine the *in vivo* role that ExaF and XoxF enzymes play in the oxidation of methanol and formaldehyde. I hypothesize that changes in carbon distribution during Ln-dependent methylotrophic growth are due to the activity of Ln-dependent enzymes, which can oxidize both methanol and formaldehyde. Further, I hypothesized that the roles of XoxF and ExaF are not interchangeable

in vivo with the primary role of XoxF1 and XoxF2 being to oxidize methanol and the primary role of ExaF being to oxidize formaldehyde. Through my work, I demonstrate the impact of Ln-dependent enzymes on the metabolic network. Phenotypic analyses allowed me to corroborate previously published work describing the biochemical capabilities of Ln-dependent MDHs as having increased oxidative capacity compared to Ca^{2+}-dependent MDHs and demonstrate the metabolic relevance of this activity.

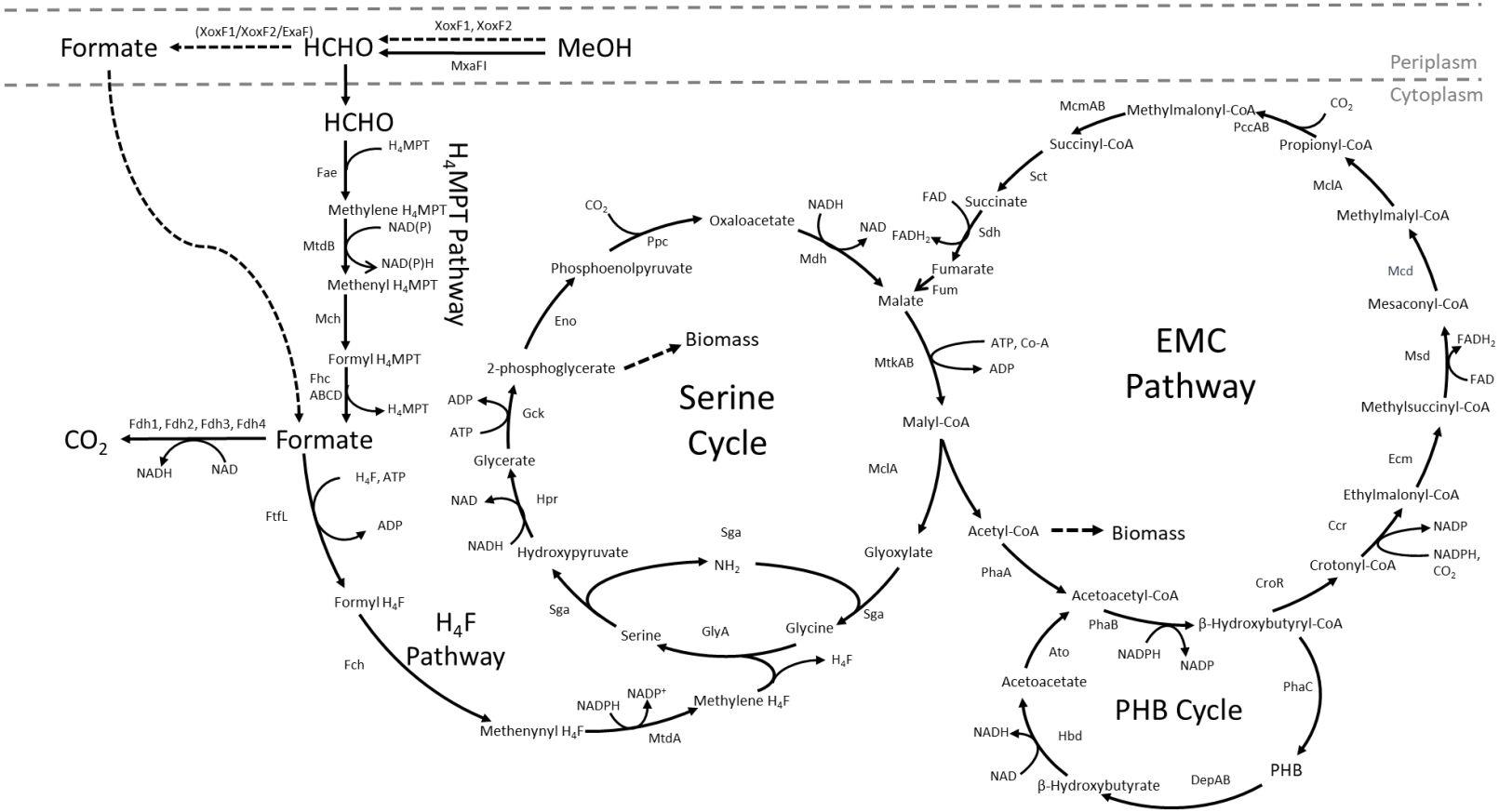

Figure 7 Methylotrophic metabolism in *M. extorquens* AM1. Abbreviations: H_4MPT, tetrahydromethanopterin, Fdh, formate dehydrogenase, H_4F, tetrahydrofolate, EMC, ethylmalonyl CoA, PHB, polyhydroxybutyrate. Fae, formaldehyde activating enzyme, MtdB, methylene-H_4MPT dehydrogenase, Mch, methenyl-H_4MPT cyclohydrolase, Fhc, formyl-H_4MPT transferase/hydrolase complex. FtfL, formyl tetrahydrofolate ligase, Fch, formyl-H_4F cyclohydrolase, MtdA, methylene-H_4MPT dehydrogenase bifunctional enzyme. GlyA, serine hydroxy methyl transferase, Sga, serine glyoxalate amino transferase, Hpr, hydroxypyruvate reductase, Gck, glycerate-2-kinase, Eno, enolase, Ppc, phosphoeonolpyruvate carboxylase, Mdh, malate dehydrogenase, MtkAB, malate thiokinase, MclA, malyl-CoA lyase. PhaA, acetyl-CoA acetyltransferase, PhaB, 3-hydroxybutryl-CoA dehydrogenase, CroR, 3-hydroxybutyryl-CoA dehydratase, Ccr, crotonyl-CoA carboxylase/reductase, Ecm, ethylmalonyl-CoA mutase, Msd, methylsuccinyl-CoA dehydrogenase, Mcd, mesaconyl-CoA hydratase, MclA, methylmalyl-CoA lyase, PccAB, propionyl-CoA carboxylase, McmAB, methylmalonyl-CoA mutase, Sct, succinyl-CoA transferase, Sdh, succinate dehydrogenase, Fum, fumarase. PhaC, poly-β-hydroxybutyrate polymerase, DepAB, poly-β-hydroxybutyrate depolymerase, Hbd, β-hydroxybutyrate dehydrogenase, Ato, acetyl-CoA/acetoacetyl-CoA transferase.

2: LANTHANIDE-DEPENDENT METHYLOTROPHIC METABOLISM LEADS TO CHANGES IN CARBON DISTRIBUTION THROUGH FORMALDEHYDE AND FORMATE METABOLIC PATHWAYS

Introduction

Methylotrophic metabolism, the ability to use reduced one-carbon compounds including methanol and methylated amines as a sole source of carbon and energy, has been studied for some 60 years (1, 5, 6). Methanol dehydrogenases (MDH) oxidize methanol to formaldehyde (24, 59). Methylotrophs then use a variety of strategies for assimilation that may be classified into broad groups according to the biochemical strategy they employ (1, 2). *Methylobacterium extorquens* AM1, a type II methylotroph, relies on the serine cycle and ethylmalonyl CoA pathway for carbon assimilation (58, 60). Formaldehyde is first oxidized to formate using the tetrahydromethanopterin (H_4MPT) pathway. Formate can either be partially reduced to methylene tetrahydrofolate (Me-H_4F) via the tetrahydrofolate pathway or oxidized by the activity of formate dehydrogenases (FDH) to CO_2 (15, 58). Me-H_4F is condensed with glycine to form serine, the first intermediate in the serine cycle (1, 58). Removal of serine cycle intermediates for assimilation, such as 2-phosophglycerate, necessitats the regeneration of glyoxyate, the precursor of serine; in most type II methylotrophs this is accomplished by the EMC pathway rather than by the glyoxylate shunt (19, 58, 61).

MDHs, responsible for the oxidation of methanol to formaldehyde, are a class of oxidoreductases found in both Gram-negative and Gram-positive bacteria (22). In Gram-negative bacteria, MDH is found in the periplasm as a pyrroloquinoline quinone (PQQ)-dependent, cytochrome-linked enzyme (22, 29). In *M. extorqens* AM1, this may be the heterotetrameric enzyme MxaFI or the dimeric XoxF enzyme (59). Each α subunit of MxaFI, encoded by *mxaF* contains one molecule of PQQ and one molecule of the divalent Lewis acid calcium (Ca^{2+}) (59).

By contrast, XoxF, while still containing PQQ, relies on a trivalent lanthanide (Ln^{3+}) for activity (26, 27, 30, 31, 35).

First described in 1995, the role of the XoxF enzyme remained cryptic for many years since biochemical characterizations suggested that its activity was not high enough to support growth on methanol, although those studies were done in the absence of Ln^{3+} (29). In 2011, Hibi *et al.* observed that Δ*mxaF* mutants were able to grow on methanol after addition of lanthanum (La^{3+}) to the media; however, they did not observe changes to transcription of either *xoxF1* or *mxaF* which contradicts later findings (30, 35). In 2012, Nakagawa *et al.* observed increased MDH activity when La^{3+}, which is chemically similar to Ca^{2+}, was added to a cell-free extract of *M. extorquens* AM1 and attributed this activity to XoxF (31). In 2014, a type 1 XoxF enzyme from *Methyloacidophilum fumariolicum* SolV was isolated, characterized, and crystallized, and found to contain the Ln cerium (Ce^{3+}) in place of Ca^{2+} (26). Further, Pol *et al.* found that Ce-XoxF can oxidize both methanol and formaldehyde potentially due to increased oxidative capacity of Ln^{3+} elements compared with Ca^{2+} (26). In 2016, it was reported that the ethanol dehydrogenase ExaF efficiently oxidizes formaldehyde in the presence of La^{3+}(28, 35). These reports demand a detailed description of changes in carbon distribution through the H_4MPT pathway to further define the role of Ln^{3+}-dependent enzymes.

In this study, I report the transcriptomic and metabolomics profile of the methylotrophic network in the presence of La^{3+} and validate changes in formate and formaldehyde metabolism when comparing growth in the presence and absence of La^{3+}.

Materials and Methods

Chemicals

Unless otherwise indicated, chemicals and enzymes were obtained from Sigma-Aldrich (St. Louis, MO, USA). Methanol and sulfuric acid were obtained from JT Baker (Avantor Performance Materials, LLC, Center Valley, Pennsylvania, USA). Nanopure (Thermo Fisher, Waltham, Massachusetts, USA) water was used for the preparation of media, buffers, standards, and samples.

Growth conditions and strains

Table 1: Strains and Plasmids used in this study

Strain or Plasmid	Description	Reference
Strain		
M. extorquens		
AM1	Rif-resistant derivative	(62)
AM1 *fae*	Δ*fae* deletion mutant	(14)
AM1 *exaF*	Δ*exaF* deletion mutant	(28)
E. coli		
BL21-AI	Electrocompetent cells	Invitrogen
Plasmid		
pNG221	pET16b with *ccr*	(18)

The strains and plasmids used in this work are summarized in Table 1. *Escherichia coli* strains were grown in 1.5 L shake flasks using lysogeny broth (LB) (BD, Franklin Lakes, NJ).

For growth on solid media, *E. coli* strains were grown on (LB) agar plates prepared with 1.5% w/v Bacto agar (BD, Franklin Lakes, NJ). *M. extorquens* AM1 strains were grown in minimal medium (63) containing 125 mM methanol unless otherwise stated using either borosilicate culture tubes or shake flasks. $LaCl_3$ was added to 2 µM for cultures containing La^{3+} (35). La^{3+}-free glassware was prepared as previously described (35). Cultures were maintained with continuous shaking at 30°C at 200 rpm. For the preparation of solid medium, minimal medium was prepared as above with 1.5% w/v Bacto agar.

To determine the minimum inhibitory concentration of methanol, *M. extorquens* strains were tested as previously described (14). Briefly, strains were patched in triplicate on solid minimal medium containing 15.5 mM succinate and the following concentrations of methanol: 125 mM, 10 mM, 1 mM, 0.1 mM, 0.01 mM, and 0.001 mM, in either the presence or absence of La^{3+}. Plates were maintained at 30°C for up to 48 hrs to allow for growth and observed for the presence or absence of growth. Growth phenotypes were monitored in liquid medium by growing three 3 mL cultures overnight in minimal media containing 15.5 mM succinate in La^{3+}-free borosilicate culture tubes. Before cultures reached stationary phase, they were harvested by centrifugation at 5000 rpm for 10 min. The supernatants were removed, and the pellets were washed by resuspension in 1 mL La^{3+}-free and carbon-free minimal medium and centrifuged again, and washed one more time. The cell pellets were resuspended in La^{3+}-free and carbon free minimal medium such that a 100 µL inoculum from this resuspension would result in a starting culture of OD_{600}=0.1 in fresh minimal medium. 100 µL of washed and resuspended culture was used to inoculate 3 mL of minimal medium containing 15.5 mM succinate in either the presence or absence of La^{3+} using La^{3+}-free borosilicate culture tubes. Cultures were grown at 30°C with continuous shaking at 200 rpm. After two hrs of growth, 100 µL of sterile methanol dilutions

were added to the following final concentrations: 125 mM, 10 mM, or 0 mM. For the 0 mM methanol concentration, 100 µL of sterile water was added. Cultures continued growth as before, and growth was monitored by measuring optical density every 3 hrs for 36 hrs using an Ultraspec 10 cell density meter at λ=600 (Amersham Biosciences, Little Chalfont, UK). Three biological replicates were used for all growth conditions.

To determine growth rates on different methanol concentrations, cultures were grown overnight on minimal medium with 15.5 mM succinate, washed and resuspended as before and used to inoculate fresh medium to an initial OD_{600} of 0.1. Media was prepared as before without succinate. Methanol concentrations used were: 125 mM, 100 mM, 75 mM, 50 mM, 25 mM. Growth was monitored every 3 hrs for 24 hrs using an Ultraspec 10 cell density meter as before.

Sample collection and storage

Unless otherwise noted, all samples were collected at an OD_{600} 0.7-0.8 by filtering 50 mL of cell culture through a Nylaflo membrane (9.75-11.23 mg total cell dry weight) (Pall Corporation, Port Washington, New York, USA) with a 0.2 µm pore size and 45 mm diameter using a vacuum filtration system. Filters were removed, placed in a pre-cooled 15 or 50 mL Falcon tube (Corning Life Sciences, Tewksbury, Massachusetts, USA) and frozen immediately in liquid nitrogen. Samples were stored for not longer than one week in a -80°C freezer before analysis unless otherwise noted.

Estimation of internal concentrations

Internal concentrations of metabolites were estimated by dividing the measured moles of metabolites (found experimentally) by the volume of cells used to make the measurement. The total volume of cells used in an assay was determined using the dry weight (0.278 g/L at

OD_{600}=1) (15), a cell volume of 36 µL/mg cell dry weight (64), average cell size of 1 by 3.2 µm (64), and average of 4 x 10^8 cells/mL at OD_{600}=1 (65).

Transcriptomics

50 ml cultures were grown in shake flasks with or without $LaCl_3$ to an OD_{600} of 0.7 that correlated with mid-exponential growth. Total RNA samples were procured, and quality was verified as previously described (18). Two biological replicates were prepared for each condition. rRNA depletion, library preparation, and Illumina Hi-Seq sequencing were performed by the Michigan State University Research Technology Support Facility (RTSF) Genomics Core. Libraries were prepared using the TruSeq Stranded Total RNA kit (Illumina, San Diego, CA), with Ribo-Zero Bacteria used for rRNA depletion (Epicentre, Madison, WI). All replicates were sequenced on an Illumina HiSeq 2500 using a multiplex strategy with 50 bp single-end reads with a target depth of >30 million mapped reads. Base calling was done by Illumina Real Time Analysis (RTA) v1.18.64 and the output of RTA was demultiplexed and converted to a FastQ format with Illumina Bcl2fastq v1.8.4. The filtered data were processed using SPARTA: Simple Program for Automated for reference-based bacterial RNA-seq Transcriptome Analysis (66). Final abundances were measured in trimmed mean of M values (TMM).

Measurement of methanol in culture supernatant

During exponential growth, culture supernatant was collected by filtering the culture through a Nylaflo membrane. 1 mL of flow-through was collected and analyzed immediately using a Shimadzu Prominence 20A series high-pressure liquid chromatography system with an SPD-20A UV-VIS detector (Shimadzu, Kyoto, Japan) and a BioRad Aminex HPX-87C organic acids column 300 x 7.8 mm with a 9 µm particle size (BioRad, Hercules, California, USA). An

isocratic flow of 5 mM HPLC grade sulfuric acid in Nanopure water was used as the mobile phase. Peak area was compared with a standard curve to determine methanol remaining in the media.

Internal concentrations of formaldehyde

To determine internal concentrations of formaldehyde, cultures were grown in minimal medium containing methanol and either the presence or absence of La^{3+}. Samples were collected by vacuum filtration and, due to the volatile nature of formaldehyde, were measured immediately. Samples were washed from the membrane by vortexing with 2 mL phosphate buffer. Filter membranes were removed and discarded. Cells were disrupted by passage once through a One Shot Cell Disruptor set to 25 PSI (Constant Systems, Ltd., Daventry, UK) and centrifuged at 13,000 rpm for 5 min. The supernatant was removed and used to measure formaldehyde using the Purpald assay (67). This end-point assay condenses formaldehyde first with the Purpald reagent (35 mM) to form an uncolored intermediate, which is oxidized by the addition of periodate (33mM) to form a purple product. The increased absorbance can be read at 550 nm. Due to an excessive accumulation of bubbles following the addition of periodate, reactions were left overnight at 4°C before transferring to plastic 96-well plates, and absorbances were read using a BioTek EpochII microplate reader (BioTek, Winooski, Vermont, USA).

Excreted and internal concentrations of formate

To measure excreted formate during growth on methanol, 50 mL of culture grown to exponential phase on minimal medium containing methanol with or without La^{3+} was filtered through a Nylaflo membrane. The membrane was discarded and the flow through was frozen immediately in liquid nitrogen and lyophilized to complete dryness. The lyophilized supernatant

was resuspended in sterile water and centrifuged for 5 min at 13,000 rpm to remove insoluble particles. The supernatant was analyzed using a Shimadzu Prominence 20A HPLC using a BioRad Aminex HPX-87C organic acids column and an isocratic flow of 5 mM sulfuric acid as for measurement of methanol mentioned above. To determine internal concentrations of formate during growth on methanol, cultures were grown on minimal medium containing methanol with or without La^{3+} and harvested as mentioned above. Cells were resuspended in 1 mL phosphate buffer, disrupted using a One Shot Cell Disruptor and centrifuged as for measurement of formaldehyde. The supernatant was removed and analyzed by a Shimadzu Prominence 20A HPLC using a BioRad Aminex HPX-87C organic acids column and an isocratic flow of 5 mM sulfuric acid as for measurement of methanol. Peak area was compared to a standard curve to determine internal concentrations.

Measurement of pyridine nucleotides

To determine internal concentrations of pyridine nucleotides, cultures were grown on methanol in minimal media in the presence or absence of La^{3+}. 25 mL cultures were harvested as previously described but immediately quenched in 1 mL of the appropriate acidic (100 mM HCl with 500 mM NaCl) or basic solution (100 mM NaOH with 500 mM NaCl) to preserve oxidized and reduced species respectively (68). Pyridine nucleotides were measured using a nucleotide cycling assay which measures both reduced and oxidized species indirectly through the phenazine ethosulfate (PES)-mediated reduction of thiazolyl blue tetrazolium and monitoring the increasing absorbance at 550 nm (68). Initial assays were performed as described previously (68) with the following modifications: 25 mL of culture was used instead of 0.75 mL, and the culture was filtered using Nylaflo membranes, PES final concentration was 0.83 mM, 0.1 U/µL of alcohol dehydrogenase was used, and final ethanol concentration was 5%. A standard curve was

constructed for each nucleotide from pure components dissolved in appropriate acid or base, which had been boiled for 5 minutes as with the samples. Standards were linear between 50 µM and 0.8 µM for most standards and between 50 µM and 0.05 µM for NADH.

Measurement of adenine nucleotides

To determine internal ratios of adenine nucleotides, cultures were grown on methanol in minimal medium in the presence or absence of La^{3+}. Cultures were harvested as previously described, quenched by freezing in liquid nitrogen and stored at -80°C for one day before processing. Samples were thawed on ice, and adenine nucleotides were extracted using a hot ethanol extraction. Briefly, samples were thawed on ice and 1 mL of a hot 75% v/v ethanol solution buffered to pH 5.2 with 70 mM HEPES was mixed with samples and were briefly vortexed to remove cells from filter membranes. Samples were incubated at 100°C for 5 min and cooled on ice for 3 min before centrifuging at 15,000 rpm for 5 min. 250 µL of sample was removed and dried using a Thermo Savant DNA 120 vacuum centrifuge (Savant Instrument, NY, USA). Samples were resuspended in 100 µL Nanopure water and analyzed using a Waters Quattro Premier XE UPLC-MS/MS tandem quadrupole mass spectrometer using a Waters Aquitiy UPLC C18 BEH 2.1 x 50 mm column with a 1.7µm pore size (Waters Corporation, Milford, MA, USA). The samples were chromatographed using a gradient of 15 mM tetrabutylammonium hydrogensulfate and 10 mM acetic acid in Nanopure water against methanol. The gradient was as follows: 0-1 min 99% aqueous phase, 1-2.5 min gradient to 80% aqueous phase, 2.4-4 min 80% aqueous phase, 4-7 min gradient to 35% aqueous phase, 7-7.5 min gradient to 5% aqueous phase, 7.5-9 min 5% aqueous phase, 9-9.1 min gradient to 99% aqueous phase, 9.1-10 min 99% aqueous phase.

Measurement of CO_2 by GC

To estimate the production of CO_2 during methylotrophic growth, cultures were grown on succinate in sealable Pyrex jars. Cultures were grown in minimal medium with 15.5 mM succinate in the presence or absence of La^{3+} as mentioned above. To ensure jars were free of La^{3+}, they were cleaned as previously described (35). When cultures reached exponential growth, 125 mM methanol was added and the containers were sealed with crimp-top glass tubes fitted in air-tight rubber fittings. Sealing cultures prevented loss of CO_2 to the environment. Using a Grace 2.5 mL gas-tight glass Luer-lock syringe (Grace Davison Discovery Science, Deerfield, IL, USA), headspace samples were removed at 0, 45, and 180 min after addition of methanol and gas composition was analyzed using a Varian CP-4900 Micro GC gas chromatography system (Chromatography Systems, Middleburg, The Netherlands). Peak areas were compared to determine relative changes in CO_2 concentrations in growth conditions. Three biological replicates and two technical replicates were used for both growth conditions.

Measurement of serine cycle and EMC pathway intermediates

To measure the accumulation of serine cycle and EMC pathway intermediates during growth on methanol, cultures were grown on methanol as mentioned above in minimal medium with methanol in the presence or absence of La^{3+}. 30 mL of culture was harvested by vacuum filtration. Metabolites were extracted using a hot extraction method to improve the stability of coenzyme-A intermediates as described previously (18). For analysis by gas chromatography, samples were derivatized with o-methoxybenzoic acid suspended to a concentration of 20 mg/mL in anhydrous pyridine and *N*-*tert*-butyldimethylsilyl-*N*-methyltrifluoroacetamide (MTBSTFA) and measured using an Agilent 5975 GC single quadrupole mass spectrometer

(Agilent Technologies, Santa Clara, California, USA). No standard curve was used, and all measurements compare growth in the absence of La^{3+} to growth in the presence of La^{3+} by comparing peak areas normalized to an internal standard of ^{13}C-labled glycine.

Coenzyme A derivatives in the EMC pathway were measured using a modification of previously described ultra-pressure liquid chromatography methods (69). Using an aqueous mobile phase of 400 mM ammonium acetate in water with 2% formic acid and an organic mobile phase of acetonitrile with 1% acetic acid and 2% formic acid with a flow rate of 0.4 mL/min, the following gradient was used: 0-1 min 98% aqueous phase, 1-3 min gradient to 95% aqueous phase, 3-5 min gradient to 60% aqueous phase, 5-6 min maintain flow at 40% aqueous phase, 6-8 min maintain flow at 98% aqueous phase. Samples were analyzed using a Waters Xevo TQ-S tandem quadrupole mass spectrometer (Waters Corporation, Milford, Massachusetts, USA) and an Acquity UPLC CSH C18 column (2.1x100 mm) with a 1.7 µm pore size (Waters Corporation, Milford, Massachusetts, USA). No standard curve was used. Samples were compared such that peak area of samples grown in the presence and absence of lanthanum were compared after normalization to an internal standard of ^{13}C-labled acetyl-CoA.

Purification of Ccr and synthesis of Ethylmalonyl-CoA

Because no commercially available ethylmalonyl-CoA standard exists, we enzymatically synthesized a standard to aid in identification of EMC pathway intermediates. Recombinant crotonyl-CoA carboxylate/reductase (Ccr) was expressed with a 10 histidine tag and purified as previously described using nickel-affinity chromatography (18). Ethylmalonyl-CoA was synthesized enzymatically as described previously using commercially available crotonyl-CoA, NADPH, and bicarbonate (20). Ethylmalonyl-CoA was purified by HPLC as previously

described, fractionating the column effluent, and combining fractions corresponding to effluent for 3 min surrounding the ethylmalonyl-CoA peak (20). In addition to obtaining relevant HPLC peaks, LC-MS/MS peaks showed that synthesized ethylmalonyl-CoA produced unique fragments compared with crotonyl-CoA.

PHB quantification via acid degradation and HPLC

Polyhydroxy butyrate (PHB) was measured as described previously (70). Briefly, cultures were grown in minimal media with methanol in the presence or absence of La^{3+} as mentioned above. During exponential growth, 50 mL of culture was harvested by centrifugation at 5000 rpm for 10 min. Culture supernatant was removed, and pellets were frozen in liquid nitrogen immediately in Falcon tubes. Pellets were dried overnight by lyophilization. Dried pellets were carefully removed from Falcon tubes being careful not to damage the plastic tubing and placed into 5 mL glass Cortex sample tubes (Corning Lifesciences, Tewksburry, MA, USA). 1 mL 18 M sulfuric acid was pipetted onto each pellet using a 1 mL Model 1001 BFP-SAL SRY salt line syringe (Hamilton Company, Reno, Nevada, USA). A glass marble was placed over the sample vial and samples were incubated at 90°C. After 1 hr, the samples were diluted 5 times with Nanopure water and analyzed using a Shimadzu Prominence 20A HPLC using a BioRad Aminex HPX-87C organic acids column and an isocratic flow of 5 mM sulfuric acid. During treatment with sulfuric acid, polyhydyroxybutyrate is degraded to crotonic acid. Therefore, standards were compared against two standard curves: one of crotonic acid and one of PHB to ensure that PHB was being degraded to crotonic acid and that crotonic acid provides an acceptable standard for measurement of PHB. Peak areas were compared to the standard curve to obtain internal concentrations of PHB.

Results

La-dependent methylotrophic transcriptomic profile

When grown with methanol in the presence of La^{3+}, *M. extorquens* AM1 exhibited a marked shift in the expression of methanol oxidation genes when compared with similar growth without Ln^{3+} (Table 2). The genes *xoxF*, *xoxG*, and *xoxJ* encoding the Ln^{3+}-dependent MDH, the predicted cognate cytochrome *c*, and a MxaJ-like protein, were all significantly upregulated. A three-gene cluster putatively encoding an ABC transporter immediately upstream of *xoxFGJ* was similarly upregulated indicating a potential role for this transport system during La^{3+}-dependent methylotrophy. Notably, *exaF*, encoding the Ln^{3+}-dependent ethanol dehydrogenase (28), was also upregulated greater than 2-fold suggesting a possible role in Ln^{3+}-dependent methylotrophy. *xoxF2* was also upregulated, although the increase in expression was less than 2-fold. In congruence with a Ln^{3+}-dependent change in methanol oxidation, the entire *mxa* gene cluster, encoding the Ca^{2+}-dependent MDH and accessory genes, was markedly downregulated, as were the genes encoding both *mxcQE* and *mxbDM*, two-component system known to be necessary for the expression of the *mxa* gene cluster (71). Several genes important for PQQ biosynthesis and processing were downregulated as well, even though XoxF1 and ExaF are PQQ-dependent dehydrogenases. Genes encoding the formaldehyde oxidizing H_4MPT pathway showed mixed responses. However, in general, the pathway was downregulated including *fae*, which encodes a formaldehyde activating enzyme.

The *M. extorquens* AM1 genome encodes at least four distinct formate dehydrogenases: *fdh1*, *fdh2*, *fdh3*, and *fdh4*, of which only *fdh4* has been demonstrated to be essential during growth on methanol (55). During La-dependent methylotrophic growth *fdh1*, *fdh2*, and *fdh3* gene

clusters were downregulated while the *fdh4* gene cluster was upregulated, indicating possible changes to formate oxidation. The H_4F pathway genes showed little change. The genes encoding the assimilatory serine cycle and the glyoxylate-replenishing EMC pathway exhibited a general trend of downregulation, although many of the expression changes were subtle. Overall, the gene expression profile of *M. extorquens* during La-dependent methylotrophy shows clear changes of genes influencing primary oxidation and both dissimilatory and assimilatory pathways, including indications of changes in formaldehyde and formate oxidation.

Table 2: Gene expression profile for La-dependent methylotrophy compared with La-independent methylotrophy in *M. extorquens* AM1

Locus tag	Gene	Description	+La (mean TMM*)	log_2 fold change (+La vs. -La)
		Methanol oxidation		
META1p1737		ABC transporter substrate binding protein (subunit A)	66	3.2
META1p1738		ABC transporter permease component (subunit B)	19	2.9
META1p1739		ABC transporter ATP-binding protein (subunit C)	38	2.9
META1p1740	*xoxF1*	lathanide-dependent methanol dehydrogenase	5415	3.0
META1p1741	*xoxG*	Cytochrome c	2090	3.6
META1p1742	*xoxJ*	conserved exported of unknown function	763	3.7
META1p2757	*xoxF2*	XoxF, PQQ-linked dehydrogenase of unknown function	248	0.8
META1p1139	*exaF*	lanthanide-dependent ethanol dehydrogenase	954	1.1
META1p4525	*mxaB*	MxaB, methanol response regulator	13	-3.3
META1p4526	*mxaH*	MxaH, predicted protein	15	-2.9
META1p4527	*mxaE*	MxaE, predicted protein	5	-4.7
META1p4528	*mxaD*	MxaD protein precursor	8	-6.3
META1p4529	*mxaL*	MxaL protein precursor	4	-5.2
META1p4530	*mxaK*	MxaK protein,membrane-associated	3	-5.5
META1p4531	*mxaC*	MxaC protein, membrane-associated	5	-4.7
META1p4532	*mxaA*	MxaA protein, membrane-associated	6	-4.0
META1p4533	*mxaS*	MxaS protein, involved in methanol oxidation	4	-5.0
META1p4534	*mxaR*	Protein MxaR (Protein MoxR)	13	-7.4
META1p4535	*mxaI*	Methanol dehydrogenase subunit 2 precursor (MDH small beta subunit)	107	-8.1
META1p4536	*mxaG*	Cytochrome c-L precursor	9	-8.5
META1p4537	*mxaJ*	MxaJ, MDH complex-associated	6	-8.5
META1p4538	*mxaF*	Methanol dehydrogenase subunit 1 precursor (MDH large alpha subunit)	115	-8.6
		PQQ Synthesis		

Table 2 (cont'd)

META1p1748	*pqqE*	Pyrroloquinoline quinone (PQQ) biosynthesis protein E	86	-2.3
META1p1749	*pqqCD*	bifunctional coenzyme pyrroloquinoline quinone (PQQ) biosynthesis protein D	114	-2.5
META1p1750	*pqqB*	Pyrroloquinoline quinone (PQQ) biosynthesis protein B	160	-1.6
META1p2330	*pqqF*	putative protease	132	-1.2
META1p4628	*pqqA*	Coenzyme pyrroloquinoline quinone (PQQ) biosynthesis protein A	463	-4.3
META1p4629	*pqqA*	Coenzyme pyrroloquinoline quinone (PQQ) biosynthesis protein A	46	-4.1
		Two-Component Regulation of *mxa* gene expression		
META1p1752	*mxbM*	two-component transcriptional regulator, response regulator	46	-1.6
META1p1753	*mxbD*	two-component transcriptional regulator, sensor kinase	63	-2.2
META1p4896	*mxcQ*	integral membrane sensor signal transduction histidine kinase	79	-0.7
META1p4897	*mxcE*	two component transcriptional regulator	40	-1.7
		H_4MPT pathway		
META1p1766	*Fae*	formaldehyde-activating enzyme	24072	-1.1
META1p1761	*mtdB*	NAD(P)-dependent methylene tetrahydromethanopterin dehydrogenase	572	0.2
META1p1763	*Mch*	N(5),N(10)-methenyl-H_4MPT cyclohydrolase	206	-0.7
META1p1755	*fhcC*	formyltransferase/hydrolase complex Fhc subunit C	134	1.0
META1p1756	*fhcD*	formyltransferase/hydrolase complex Fhc subunit D	393	0.0
META1p1757	*fhcA*	formyltransferase/hydrolase complex Fhc subunit A	417	-0.8
META1p1758	*fhcB*	Formyltransferase/hydrolase complex Fhc subunit B	396	1.1
		Formate dehydrogenases		
META1p5031	*fdh1B*	Tungsten-containing formate dehydrogenase beta subunit	317	-1.4
META1p5032	*fdh1A*	Tungsten-containing formate dehydrogenase alpha subunit	460	-1.8
META1p4847	*fdh2B*	NAD-dependent formate dehydrogenase, Molybdenum containing, beta subunit	104	-0.9
META1p4848	*fdh2A*	NAD-dependent formate dehydrogenase, molybdenum containing, alpha subunit	273	-1.2
META1p0303	*fdh3A*	formate dehydrogenase alpha subunit precursor (tat pathway signal)	673	-1.4
META1p0304	*fdh3B*	Formate dehydrogenase iron-sulfur (beta) subunit	155	-1.4
META1p0305	*fdh3C*	Formate dehydrogenase gamma (cytochrome) subunit	256	-1.0
META1p2093	*fdh4B*	Formate dehydrogenase subunit B	34	2.2
META1p2094	*fdh4A*	Formate dehydrogenase subunit A	229	1.9
		H_4F pathway		
META1p0329	*ftfL*	formate-tetrahydrofolate ligase (formyltetrahydrofolate synthetase)	1374	-0.6
META1p1729	*Fch*	methenyl tetrahydrofolate cyclohydrolase	815	-0.1
META1p1728	*mtdA*	NADP-dependent methylene-H_4MPT/H_4F dehydrogenase	1682	0.1
		Serine Cycle		
META1p3384	*glyA*	serine hydroxymethyltransferase	2234	-0.5
META1p1726	*Sga*	serine-glyoxylate aminotransferase (SGAT)	3650	-0.2
META1p1727	*hprA*	Hydroxypyruvate reductase, NAD(P)H-dependent	779	-0.3
META1p2944	*Gck*	glycerate kinase	347	0.8

Table 2 (cont'd)

META1p2984	*Eno*	Enolase	498	-0.5
META1p1732	*ppc*	phosphoenolpyruvate carboxylase	1310	-0.1
META1p1537	*Mdh*	malate dehydrogenase	271	-0.5
META1p1730	*mtkA*	Malate thiokinase, large subunit	1683	-0.4
META1p1731	*mtkB*	Malate thiokinase, small subunit	990	-0.3
META1p1733	*mcl*	malyl-CoA lyase/beta-methylmalyl-CoA lyase	2509	-0.1
		EMC Pathway		
META1p3700	*phaA*	beta-ketothiolase	494	-0.4
META1p3701	*phaB*	acetoacetyl-CoA reductase	1396	-0.4
META1p3675	*croR*	Crotonase	141	-0.3
META1p0178	*ccr*	crotonyl-CoA carboxylase/reductase	2025	0.0
META1p0839	*Epi*	ethylmalonyl-CoA/methylmalonyl-CoA epimerase	111	-1.2
META1p0180	*Ecm*	ethylmalonyl-CoA mutase	678	-0.1
META1p4153	*Mcd*	Mesaconyl-CoA hydratase	357	-0.6
META1p2223	*Msd*	Methylsuccinyl-CoA dehydrogenase	328	-0.8
META1p0172	*pccB*	propionyl-CoA carboxylase beta chain	733	-0.9
META1p3203	*pccA*	propionyl-CoA carboxylase alpha subunit	720	-0.3
META1p0188	*mcmB*	methylmalonyl-CoA mutase accessory protein	68	0.6
META1p1433	*mcmA*	cobalamin adenosyltransferase	39	-1.0
META1p1538	*sucC*	succinyl-CoA synthetase, beta subunit	336	-0.8
META1p1539	*sucD*	succinyl-CoA synthetase, alpha subunit	238	-0.3
META1p1540	*sucA*	2-oxoglutarate dehydrogenase complex, E1 component	603	-0.5
META1p1541	*sucB*	dihydrolipoamide succinyltransferase	224	-0.7
META1p3859	*sdhC*	succinate dehydrogenase, cytochrome b556 subunit	93	-0.1
META1p3860	*sdhD*	Succinate dehydrogenase delta subunit	60	0.3
META1p3861	*sdhA/B*	succinate dehydrogenase, flavoprotein subunit	210	0.1
META1p3863	*sdhB*	succinate dehydrogenase, iron-sulfur subunit	177	-0.4
META1p2857	*fumC*	fumarase C	158	-1.2
		PHB cycle		
META1p3304	*phaC*	Poly(3-hydroxyalkanoate) polymerase (PHA synthase)	128	-0.9
META1p4148		intracellular PHB depolymerase, polyhydroxyalkanoate depolymerase	127	-1.1
META1p4189		putative Poly(3-hydroxybutyrate) depolymerase	35	-0.5
META1p4597	*depB*	PHB depolymerase	49	-0.4
META1p0419	*depA*	intracellular PHB depolymerase	79	-0.4
META1p1376		putative Poly(3-hydroxybutyrate) depolymerase	20	1.7
META1p1436	*hbdA*	3-hydroxybutyryl-CoA dehydrogenase	436	0.0
META1p5182	*Hbd*	D-beta-hydroxybutyrate dehydrogenase	106	-0.7
META1p3124	*atoD*	acetyl-CoA:acetoacetyl-CoA transferase, alpha subunit	195	-0.2
META1p3125	*atoA*	acetyl-CoA:acetoacetyl-CoA transferase, beta subunit	127	-0.6

* trimmed mean of M values

Oxidation of methanol to formaldehyde

Previous work has demonstrated the ability of Ln^{3+}-dependent systems, including XoxF and ExaF, to oxidize methanol to formaldehyde (26, 28). In the XoxF enzyme of *M. fumariolicum* SolV, the use of lanthanides has been proposed to increase the oxidation capacity allowing for oxidation of both methanol and formaldehyde by the same enzyme and biochemical characterization has shown that this XoxF can efficiently oxidize both substrates (26). RNAseq

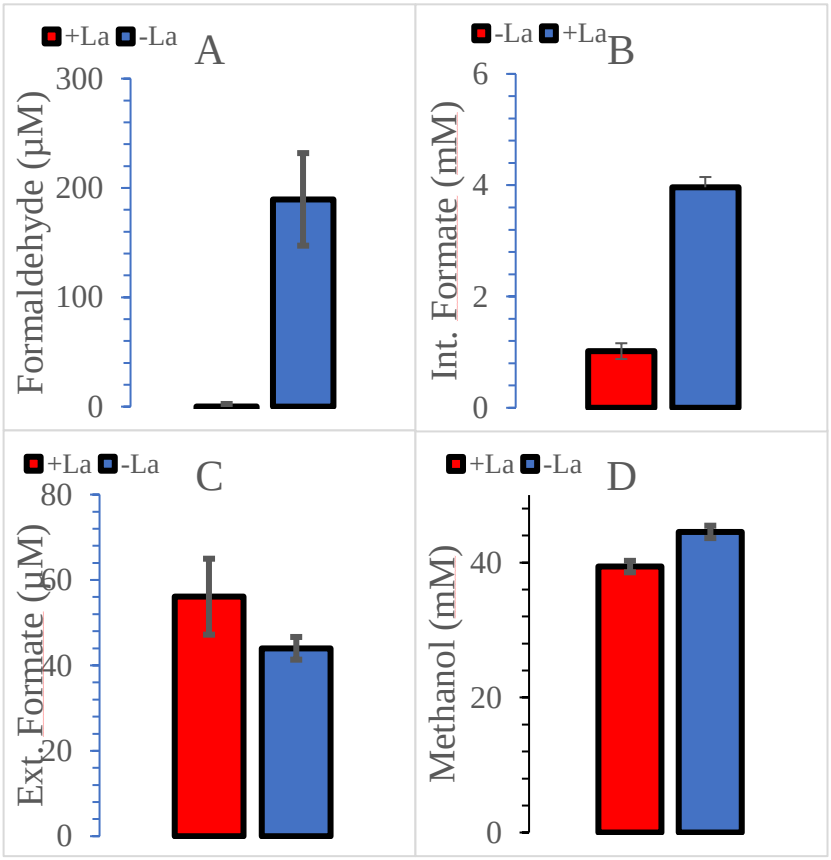

Figure 8 Formaldehyde and formate concentrations and methanol consumption for La^{3+}-dependent vs. La^{3+}-independent growth with methanol. (A) Internal concentration of formaldehyde. The $-La^{3+}$ average was 189 µM while formaldehyde was undetectable in the $+La^{3+}$ samples (student's t-test p=0.01). (B) Internal concentration of formate. The $–La^{3+}$ average was 1.01 mM while the $+La^{3+}$ average was 3.96 mM (student's t-test p=2.46E-4) (C) Excreted formate concentration in spent media. $+La^{3+}$ average was 56.1 µM while the $–La^{3+}$ average was 43.9 µM (student's t-test p=0.139). (D) Methanol consumption from spent media. $+La^{3+}$ average was 39.4 mM consumed while $–La^{3+}$ average was 44.5 mM (student's t-test p=2.49E-4). Data represents three biological replicates with two technical replicates for each sample. Error bars represent standard error or the mean. Samples were collected at OD_{600}≈0.8.

showed that transcripts of both *xoxF* and *exaF* were upregulated at least two-fold in the presence of La^{3+} while transcripts of the entire *mxa* operon were downregulated compared to levels in cells grown in the absence of La^{3+}. So, I analyzed changes in carbon distribution through oxidation of methanol in the presence of La^{3+}. Growth in the absence of La^{3+} showed accumulation of formaldehyde to an internal concentration of approximately 200 µM; however, formaldehyde was undetectable during growth in the presence of La^{3+} (Figure 8). The lower limit of detection for formaldehyde by the Purpald assay was 50 µM as determined by titration. Since changes to the accumulation of formaldehyde may be due to changes in consumption of methanol, the amount of methanol consumed from culture supernatant was measured, and no biologically significant difference was found: 39.4 mM ± 0.85 SEM compared with 44.5 mM ± 0.92 SEM in the presence and absence of La^{3+} respectively (Figure 8).

Oxidation of formaldehyde to formate

Previous work has demonstrated biochemically the ability of some XoxF enzymes and the ExaF enzyme from *M. extorquens* AM1 to oxidize formaldehyde to formate providing a potential alternative to the H_4MPT pathway (26, 28). To determine if this biochemical ability had a physiological impact, I compared the accumulation of formate during growth on methanol in the presence and absence of La^{3+} and found a 4-fold increase in accumulation of formate during growth in the presence of La^{3+}, 3.96 mM ± 0.18 mM SEM in the presence of La^{3+} compared with 1.01 mM ± 0.14 mM SEM in the absence of La^{3+} (Figure 8). However, because *M. extorquens* AM1 may excrete formate to avoid a toxic accumulation, formate concentrations were also determined in culture supernatant, and no significant difference was found: 56.1 µM ± 8.8 µM SEM compared with 43.9 µM ± 0.2 µM SEM in the presence and absence of La^{3+} respectively (Figure 8). I, therefore, hypothesized that this change in the distribution of carbon was due to the

availability of an alternative pathway for oxidation of formaldehyde. To test this possibility, I compared changes in sensitivity of mutants to the minimum inhibitory concentration (MIC), of methanol because growth on methanol correlates with formaldehyde accumulation (14). In the absence of La^{3+}, a Δ*fae* mutant has a MIC of 10 mM methanol when grown on succinate (14) (Figure 9). In the presence of La^{3+}, sensitivity to methanol decreased such that the MIC exceeds 125 mM methanol (Figure 9).

To determine if changes to the MIC of the Δ*fae* mutant were due to the availability of an alternative pathway, we examined internal formaldehyde levels during growth in the presence

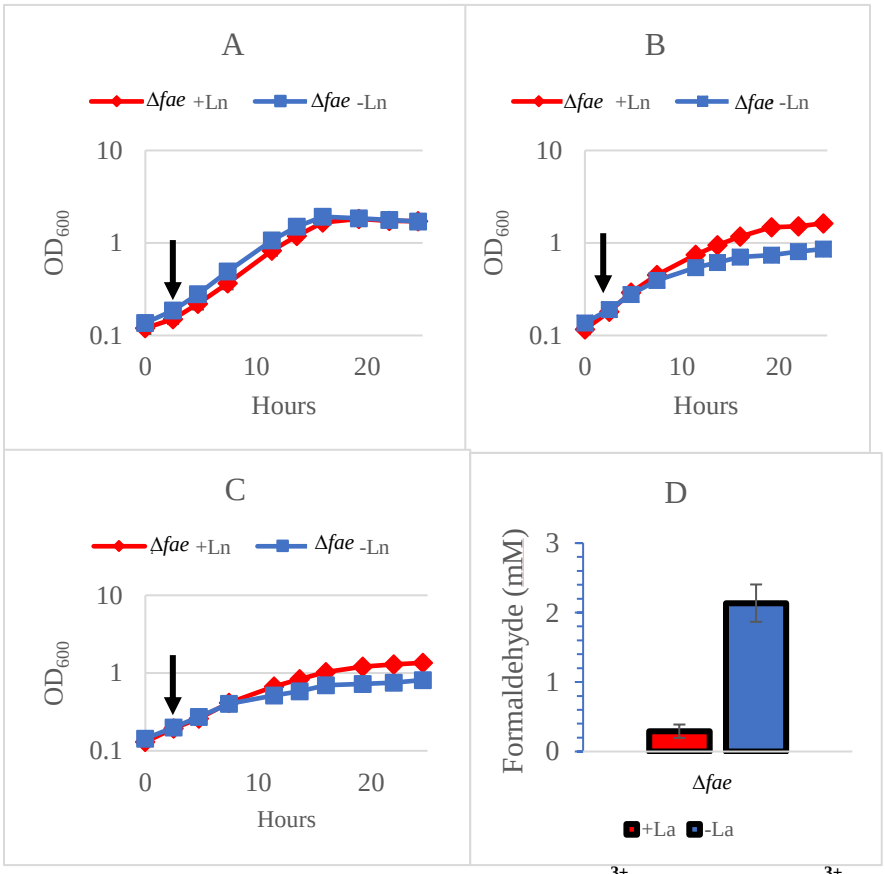

Figure 9 Changes to sensitivity of a Δ*fae* mutant during La^{3+}-dependent vs La^{3+}-independent growth on succinate and internal concentrations of formaldehyde. (A) Growth with 0 mM methanol and 15.5 mM succinate. (B) Growth with 10 mM methanol and 15.5 mM succinate. (C) Growth with 125 mM methanol and 15.5 mM succinate. Cultures were grown for two hours with succinate before addition of methanol represented by black arrow. Error bars represent SEM of three biological replicates. Black arrows indicate addition of methanol to cultures. (D) Internal concentration of formaldehyde in a Δ*fae* mutant grown on succinate and 10 mM methanol. $+La^{3+}$ average was 2.13 mM while the –La average was 0.292 mM (student's t-test p=3.09E-3).

and absence of La^{3+} when grown on 10 mM methanol and 15.5 mM succinate. The Δ*fae* mutant does not grow on methanol alone in the presence or absence of La^{3+} (data not shown). When grown on succinate and 10 mM methanol, a Δ*fae* mutant accumulates approximately 7-fold less formaldehyde in the presence of La^{3+}: 0.292 mM compared with 2.13 mM in the presence and absence of La^{3+}, respectively (Figure 9).

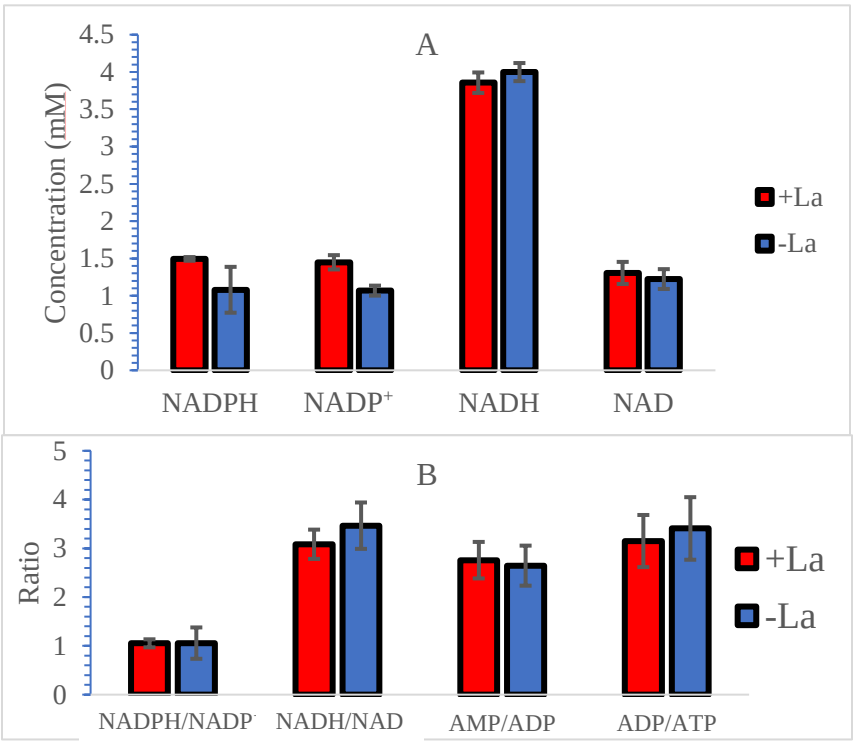

Figure 10 Internal concentrations of pyridine nucleotides and ratios of reduced vs oxidized pyridine nucleotides and phosphorylated adenine nucleotides during growth on MeOH in the presence of La^{3+} and absence of La^{3+}. (A) Internal concentrations of pyridine nucleotides for wild type *M. extorquens* AM1 cultures grown in the presence and absence of La^{3+}. For NADPH, the $+La^{3+}$ average was 1.49 mM and the $–La^{3+}$ average was 1.08 mM (student's t-test p=0.144). For $NADP^+$, the $+La^{3+}$ average was 1.44 mM and the $–La^{3+}$ average was 1.07 mM (student's t-test p=0.0153). For NADH, the $+La^{3+}$ average was 3.86 mM and the $–La^{3+}$ average was 3.99 mM (student's t-test p=0.263). For NAD^+, the $+La^{3+}$ average was 1.31 mM and the $–La^{3+}$ average was 1.22 mM (student's t-test p=0.367). (B) Ratio of reduced to oxidized pyridine nucleotides and ratios of phosphorylated adenine nucleotides. For $NADPH/NADP^+$, the $+La^{3+}$ ratio was 1.05 and the $–La^{3+}$ average was 1.06 (student's t-test p=0.496). For $NADH/NAD^+$, the $+La^{3+}$ ratio was 3.08 and the $–La^{3+}$ ratio was 3.46 (student's t-test p=0.289). For AMP/ADP, the $+La^{3+}$ ratio was 2.76 and the $–La^{3+}$ ratio 2.64 (student's t-test p=0.429). For ADP/AMP, the $+La^{3+}$ ratio was 3.15 and the $–La^{3+}$ ratio was 3.41 (student's t-test p=0.392). Samples were collected at OD_{600}≈0.8. Error bars represent SEM of two biological and two technical replicates.

Accumulation of Pyridine and Adenine Nucleotides

In the absence of La^{3+}, formaldehyde is oxidized by the H_4MPT pathway to produce formate and reduce $NAD(P)^+$ (2, 72). Known La^{3+}-dependent enzymes are PQQ-dependent MDH's and are believed to produce ATP suggesting that oxidation of formaldehyde by these enzymes would result in formate and ATP rather than making formate and reducing $NAD(P)^+$ (26, 28). I investigated potential changes to internal concentrations of the various pyridine nucleotides during growth in the presence and absence of La^{3+}. I found no significant changes to internal concentrations of pyridine nucleotides (Figure 10). Additionally, we found no significant changes to ratios of NAD/NADH, NADP/NADPH, AMP/ADP, or ADP/ATP (Figure 10).

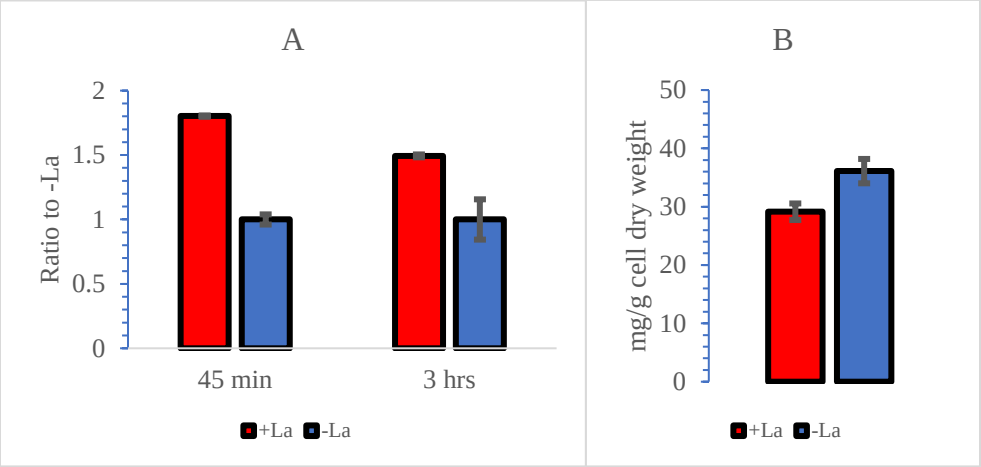

Figure 11 Ratios of CO_2 production and accumulation of PHB in the presence and absence of La^{3+}. (A) CO_2 production 45 min and 3 hrs after addition of methanol. Cultures were grown to an OD_{600}≈0.8 on 15.5 mM succinate before 125 mM methanol was added and cultures were sealed to prevent loss of CO_2 to the ambient atmosphere. Ratios of CO_2 accumulation are compared to cultures grown in the absence of La^{3+}. After 45 min, the ratio represented a 1.82-fold increase in CO_2 accumulation (student's t-test p=5.16E-4). After 3 hrs, the ratio represented a 1.49-fold increase in CO_2 accumulation (student's t-test p=0.0309). (B) Accumulation of intracellular PHB during growth in the presence or absence of La^{3+}. In the presence of La^{3+}, PHB accumulates to 29.4 mg/g cell dry weight while growth in the absence of La^{3+} accumulates PHB to 36.1 mg/g cell dry weight (student's t-test p=0.0175). Cultures for PHB measurement were grown to an OD_{600}≈0.8 before harvesting. Error bars for both CO_2 and PHB represent SEM of three biological and two technical replicates.

Carbon Distribution in the Serine Cycle and EMC Pathways

During methylotrophic metabolism in *M. extorquens* AM1, 70% of formate is oxidized to CO_2 while the remaining 30% is partially reduced to methylenetetrahydrofolate (Me-H_4F) and assimilated through the serine cycle and EMC pathways (15, 58). To determine if changes in the accumulation of formate altered the split of formate between oxidation and assimilation, we used targeted metabolomic techniques to examine changes in production of CO_2 and accumulation of intermediates in the serine cycle and EMC pathway. CO_2 production increased 1.8-fold in the presence of La^{3+} suggesting possible changes to the split between assimilation and oxidation of formate (Figure 11).

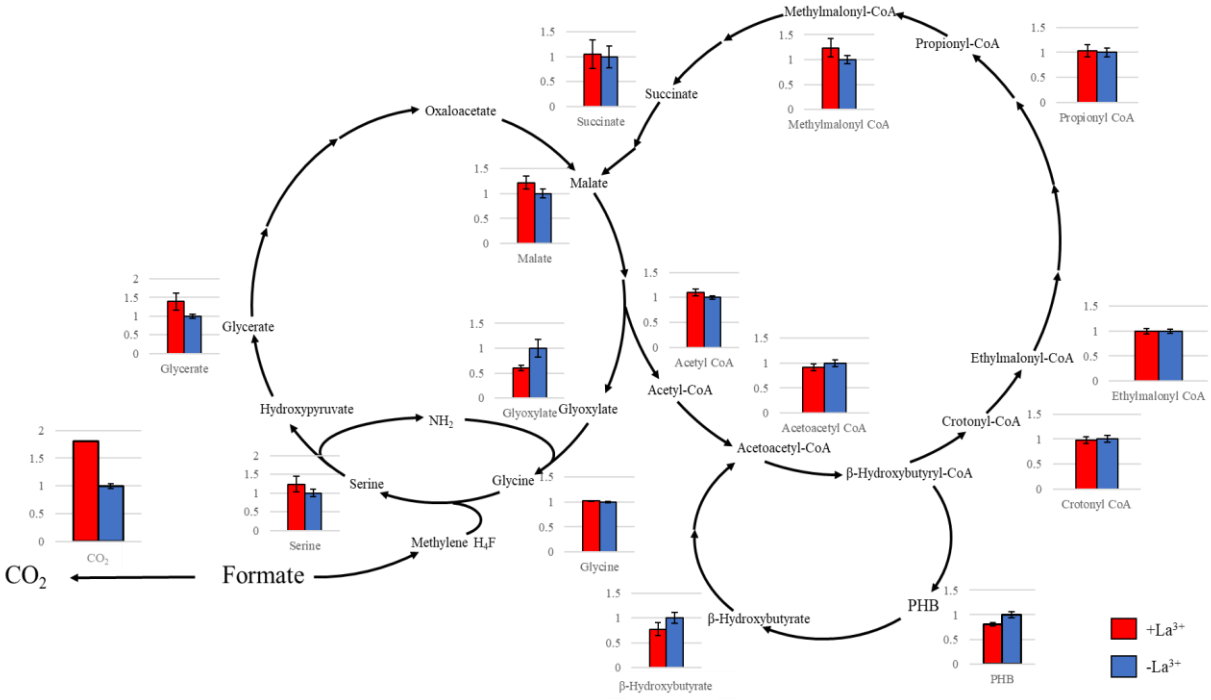

Figure 12 Ratios of intermediates in carbon assimilation pathways in the presence of La^{3+} compared with the absence of La^{3+}. Growth in the presence of La^{3+} is shown in red while growth in the absence of La^{3+} is shown in blue. Samples were collected at OD_{600}≈0.8. CoA derivatives were measured using LC-MS/MS. PHB was measured using acid degradation and HPLC. CO_2 was measured using GC-FID and data shown represents the ratio found at 45 min. All other intermediates were measured using GC-MS. Error bars represent SEM with at least three biological replicates.

Some organisms use a linear PHB cycle which converts acetyl-CoA to PHB though three steps: condensation of two acetyl-CoA molecules to form acetoacetyl-CoA, reduction of acetoacetyl-CoA to β-hydroxybutyrl-CoA, and polymerization of β-hydroxybutyryl-CoA into PHB (73). In these organisms, accumulation of PHB can be used as a form of energy or carbon storage (73). However, type II methylotrophs use a PHB cycle in which PHB is polymerized and depolymerized by separate enzymes (Figure 7). This has been hypothesized to be a useful mechanism for redox balancing where PHB can act as an alternative electron acceptor (74). PHB was quantified using acid degradation, measured by HPLC and found to accumulate slightly less during growth in the presence of La^{3+} (Figure 11). A slight, but statistically significant, decrease in the accumulation of PHB of 20% was found during growth in the presence of La^{3+}.

The serine cycle and EMC pathway showed few changes during growth in the presence of La^{3+} (Figure 12). Glyoxylate showed an almost 2-fold decrease in accumulation during growth in the presence of La^{3+}. However, this change did not reach statistical significance (student's t-test p=0.079) (Figure 12). Glyoxylate is a toxic but necessary intermediate in the serine cycle responsible for serving as an amino group acceptor to produce glycine which, in turn, acts as an acceptor for methylene-H_4F (2, 58).

Discussion

Metagenomic analysis of methylotrophic communities has revealed that many potential methylotrophs possess *xoxF* while lacking the more canonical *mxaF*. It has also been shown that the *xoxF* gene is widespread in the environment (3). From Pol *et al.*(26) and Good *et al.*(28) it is clear that the biochemical capabilities of Ln-dependent enzymes provide a potential physiologically relevant method for oxidation of formaldehyde independently of more well-known modules such as the H_4MPT pathway. In this study, I investigated the potential role Ln-

dependent enzymes may play physiologically during methylotrophic metabolism using systems-level approaches including transcriptomics and metabolomics and found changes in the accumulation of formate and formaldehyde during methylotrophic growth in the presence of Ln. I also tested the ability of Ln-dependent enzymes to oxidize formaldehyde in the absence of the H_4MPT pathway and found that sensitivity to methanol metabolism decreased in the presence of La^{3+} suggesting that at least one Ln-dependent enzyme oxidizes formaldehyde in a physiologically relevant manner.

Changes in global gene transcription comparing methanol growth in the presence and absence of La^{3+} corroborated the transcriptional effect previously reported in which the expression of *xoxF* has been demonstrated to be necessary for expression of some *mxaF* (35, 71). As expected, transcription of the *xoxF* operon was upregulated while transcription of *mxa* genes was down-regulated (Table 2) (35). Additionally, transcription of *mxcE, mxbD* and *mxbM* were all down-regulated consistent with previous findings from Skovran *et al.* which suggested that MxbDM may play either a direct or indirect role in regulating expression of *xoxF* and that MxcQE is needed for expression of *mxbDM* (Table 2) (71). Changes to transcription in the presence of La^{3+} suggest that high levels of *xoxF* expression leads to down-regulation of *mxcQE* leading to down-regulation of *mxbDM* which leads to downregulation of *mxa* genes. It is possible, therefore, that the effect of La^{3+} on transcription of *xox* genes is due to an interaction of La^{3+} with MxbM that prevents it from inhibiting *xoxF* transcription or interacting with some downstream inhibitor of *xox* gene expression.

We also saw significant changes to the expression of formate dehydrogenase enzymes. Expression of operons for *fdh1, fdh2,* and *fdh3* were all downregulated in the presence of La^{3+} while expression from the *fdh4* operon was upregulated (Table 2). Although actual counts of

transcripts for the *fdh4* genes are low in comparison to other *fdh* genes, we know from changes to the expression of *exaF*, which has similarly low counts but is upregulated 1.6-fold, that fold changes in transcription of genes with low transcription counts in an RNAseq profile may still represent physiologically relevant changes (28, 35). Changes of expression of *fdh4* are also of interest because it has been previously suggested that *fdh4* is required for expression of *fdh1*, *fdh2*, and *fdh3* genes, although characterization of this enzyme has not yet been successful (55). Mutants expressing only *fdh4* transiently excrete formate early in growth on methanol but mutants lacking either *fdh4A* or *fdh4B* experienced a growth arrest during growth on methanol and high accumulation of formate suggesting that Fdh4 is the predominant Fdh for methylotrophic metabolism (55, 57). Changes to the production of CO_2 and *fdh* gene transcription in the presence of La^{3+} may suggest that *fdh4* is under the direct or indirect control of Ln or that changes to carbon distribution resulting from the activity of XoxF1, XoxF2 and ExaF results in changes to the expression of *fdh4* which leads to changes in production of CO_2. It may also suggest that transcription of *fdh4* directly or indirectly influences transcription of *fdh1*, *fdh2*, and *fdh3*.

No significant changes were seen in the expression of genes involved in carbon assimilation cycles, which was corroborated by metabolomic data. Although no change in carbon accumulation through assimilation pathways was found in the presence of La^{3+}, this does not imply that changes to carbon flux are not present, since it has been shown that changes to flux may show little or no change in of accumulation of metabolic intermediates. Changes to the production of CO_2, expression of *fdh* genes, and accumulation of formaldehyde and formate suggest that some change to carbon flux is occurring in the presence of La^{3+} even if it is not evident in carbon distribution through the serine cycle and EMC pathway.

The metabolomic profile in the presence of La^{3+} showed few changes except to accumulation of formate and formaldehyde in the presence of La^{3+} and production of CO_2. I, therefore, hypothesized that some combination of XoxF1, XoxF2, ExaF, and the H_4MPT pathway were responsible for the oxidation of formaldehyde in the presence of La^{3+}. Our results show that, while the H_4MPT pathway is not dispensable for methylotrophic growth since Δ*fae* mutants were only able to grow on methanol in the presence of succinate regardless of the presence or absence of La^{3+} (data not shown), sensitivity to the accumulation of methanol metabolism intermediates is significantly decreased in the presence of La^{3+} suggesting that some combination of XoxF1, XoxF2 and ExaF are responsible for the oxidation of formaldehyde physiologically. Biochemical data for ExaF suggests that it may be responsible for the oxidation of formaldehyde physiologically, although further tests will need to be conducted to test this hypothesis (28).

3: CONCLUSIONS AND FUTURE DIRECTIONS

This study demonstrates the impact of Ln^{3+}-dependent enzymes on the metabolic and transcriptomic profile of *M. extorquens* AM1. I have shown that Ln^{3+} have a significant impact on global gene regulation with respect to methylotrophic metabolism and that expression of Ln-dependent enzymes results in changes to carbon distribution through primary oxidation pathways. Further, I have demonstrated the ability of Ln^{3+}-dependent enzymes to oxidize formaldehyde independently of the H_4MPT pathway. Changes to the expression of *fdh* genes, production of CO_2, and accumulation of formate may suggest there may be changes to carbon flux through Ln^{3+}-dependent methylotrophy in comparison with flux through non-Ln dependent modules and a more detailed study is warranted.

Changes to the expression of *fdh4* particularly, a relatively uncharacterized enzyme, in conjunction with changes to CO_2 production demand further investigation into the biochemical capabilities of this enzyme. Previous attempts to characterize Fdh4 were unable to identify an electron acceptor through standard biochemical tests (55). Genetics of *fdh4* do not suggest the use of a dedicated cytochrome, as for Fdh3, and biochemical tests were unable to confirm dependence on NAD^+ for activity as for Fdh1 and Fdh2 (55). This result may mean that Fdh4 uses an unknown electron acceptor or that standard biochemical tests were unable to detect NAD^+-dependence due to other unique characteristics of the enzyme. It is also possible that either Fdh4A or Fdh4B can directly or indirectly influence the transcription of *fdh1*, *fdh2*, and *fdh3* genes and this possibility should be further pursued.

Despite previous findings in *M. fumariolicum* SolV that some XoxF oxidize both methanol and formaldehyde, this may not be true for all isoforms of the enzyme. Unpublished

results from our lab suggest that activity of XoxF from *M. extorquens* AM1 may not be able to oxidize formaldehyde efficiently enough to provide physiological relevance. However, ExaF has been shown to be a very efficient formaldehyde dehydrogenase and can support growth on methanol in the absence of other known MDHs (28). Phenotypic results from mutants expressing ExaF as the only MDH also suggest that the primary role of ExaF during methylotrophic growth is not oxidation of methanol since growth rate is greatly reduced but does not appear to be limited by toxicity (28). It is therefore likely that the roles of individual Ln^{3+}-dependent enzymes are not interchangeable during methylotrophic metabolism. This hypothesis requires further investigation and will be important in defining the physiological role of each enzyme during methylotrophy.

Understanding the function of Ln^{3+} enzymes in methylotrophic metabolism provides greater insights into the roles methylotrophs may play in the environment by defining what their biochemical capabilities are and under what circumstances organisms possessing these enzymes are likely to grow. Additionally, Ca^{2+} is a widely used coenzyme and defining the differences Ln^{3+}-dependent enzymes have in comparison with their Ca^{2+}-dependent homologs may provide greater insight into potential roles for Ln^{3+}-dependent enzymes and aide in identification of potential targets for further investigation.

APPENDIX

Table 3: Table of Reprint Licenses

Figure	Original Author	Publisher	License Number
1	Qiang *et al.*, 2014	Elsevier	4140841206543
2	Qiang *et al.*, 2014	Elsevier	4140841206543
3	Brigham *et al.*, 2017	Springer	4140881261627
4	Gosh *et al.*, 1995	Elsevier	4140430976309
4	Blake *et al*., 1994	Nature Publishing Group	4140440609577
4	Pol *et al*., 2014	John Wiley and Sons	4140450935295
4	Good *et al*., 2016	American Society of Microbiology	No license necessary*
5	Keltjens *et al*., 2014	Springer	4140540965405
6	Leopoldini *et al*., 2007	John Wiley and Sons	4140461024986

*Because reuse of this figure is for use in a thesis or dissertation, ASM does not require a specific license number.

BIBLIOGRAPHY

BIBLIOGRAPHY

1. Anthony C. 1982. The biochemistry of methylotrophs. Trends in Biochemical Sciences. Academic Press, New York NY.

2. Chistoserdova L. 2011. Modularity of methylotrophy, revisited. Environ Microbiol 13:2603–22.

3. Taubert M, Grob C, Howat AM, Burns OJ, Dixon JL, Chen Y, Murrell JC. 2015. XoxF encoding an alternative methanol dehydrogenase is widespread in coastal marine environments. Environ Microbiol 17:3937–48.

4. Vorholt JA. 2012. Microbial life in the phyllosphere. Nat Rev Microbiol 10:828–40.

5. Large PJ, Peel D, QuayleE JR. 1961. Microbial growth on C1 compounds. 2. Synthesis of cell constituents by methanol- and formate-grown *Pseudomonas* AM 1, and methanol-grown *Hyphomicrobium vulgare*. Biochem J 81:470–80.

6. Peel D, Quayle JR. 1961. Microbial growth on C1 compounds. 1. Isolation and characterization of *Pseudomonas* AM 1. Biochem J 81:465–9.

7. Day DJ, Anthony C. 1990. Methanol Dehydrogenase from *Methylobacterium extorquens* AM1. Methods Enzymol 188:210–216.

8. Chistoserdova L, Lidstrom M. 2013. Aerobic Methylotrophic Prokaryotes, p. 267–285. *In* Rosenberg, E, DeLong, EF, Thompson, F, Lory, S, Stackebrandt, E (eds.), The Prokaryotes, 4th ed. Springer Berlin Heidelberg, Berlin, Heidelberg, Germany.

9. Boden R, Kelly DP, Murrell JC, Sch?fer H. 2010. Oxidation of dimethylsulfide to tetrathionate by *Methylophaga thiooxidans* sp. nov.: a new link in the sulfur cycle. Environ Microbiol 12:2688-2699.

10. Fulton GL, Nunn DN, Lidstrom ME. 1984. Molecular cloning of a malyl coenzyme A lyase gene from *Pseudomonas sp.* strain AM1, a facultative methylotroph. J Bacteriol 160:718–23.

11. Fei Q, Guarnieri MT, Tao L, Laurens LMLL, Dowe N, Pienkos PT. 2014. Bioconversion of natural gas to liquid fuel: Opportunities and challenges. Biotechnol Adv 32:596–614.

12. Anthony C. 2011. How half a century of research was required to understand bacterial growth on C_1 and C_2 compounds; the story of the serine cycle and the ethylmalonyl-CoA pathway. Sci Prog 94:109–137.

13. Vorholt JA, Marx CJ, Lidstrom ME, Thauer RK. 2000. Novel formaldehyde-activating enzyme in *Methylobacterium extorquens* AM1 required for growth on methanol. J Bacteriol 182:6645–6650.

14. Marx CJ, Chistoserdova L, Lidstrom ME. 2003. Formaldehyde-detoxifying role of the

tetrahydromethanopterin-linked pathway in *Methylobacterium extorquens* AM1. J Bacteriol 185:7160–8.

15. Crowther GJ, Kosály G, Lidstrom ME. 2008. Formate as the main branch point for methylotrophic metabolism in *Methylobacterium extorquens* AM1. J Bacteriol 190:5057–62.

16. Marx CJ, Laukel M, Vorholt JA, Lidstrom ME. 2003. Purification of the formate-tetrahydrofolate ligase from *Methylobacterium extorquens* AM1 and demonstration of its requirement for methylotrophic growth. J Bacteriol 185:7169–75.

17. Dunstan PM, Anthony C. 1972. Microbial Metabolism of C1 and C2 Compounds. Biochem J 128:107–115.

18. Good NM, Martinez-Gomez NC, Beck DAC, Lidstrom ME. 2015. Ethylmalonyl coenzyme A mutase operates as a metabolic control point in *Methylobacterium extorquens* AM1. J Bacteriol 197:727–35.

19. Peyraud R, Kiefer P, Christen P, Massou S, Portais J, Vorholt JA. 2009. Demonstration of the ethylmalonyl-CoA pathway by using ^{13}C metabolomics. Proc Natl Acad Sci USA 106:4846–51.

20. Erb TJ, Rétey J, Fuchs G, Alber BE. 2008. Ethylmalonyl-CoA mutase from *Rhodobacter sphaeroides* defines a new subclade of coenzyme B12-dependent acyl-CoA mutases. J Biol Chem 283:32283–93.

21. Kim BH, Gadd GM. 2008. Bacterial Physiology and Metabolism. Cambridge University Press, Cambridge, UK.

22. Anthony C. 2004. The quinoprotein dehydrogenases for methanol and glucose. Arch Biochem Biophys 428:2–9.

23. Hektor HJ, Kloosterman H, Dijkhuizen L. 2000. Nicotinoprotein methanol dehydrogenase enzymes in Gram-positive methylotrophic bacteria. J Mol Catal - B Enzym.

24. Goodwin PM, Anthony C. 1998. The biochemistry, physiology and genetics of PQQ and PQQ-containing enzymes. Advances in microbial physiology.

25. Williams P a, Coates L, Mohammed F, Gill R, Erskine PT, Coker a, Wood SP, Anthony C, Cooper JB. 2005. The atomic resolution structure of methanol dehydrogenase from *Methylobacterium extorquens*. Acta Crystallogr D Biol Crystallogr 61:75–9.

26. Pol A, Barends TRM, Dietl A, Khadem AF, Eygensteyn J, Jetten MSM, Op den Camp HJM. 2014. Rare earth metals are essential for methanotrophic life in volcanic mudpots. Environ Microbiol 16:255–64.

27. Keltjens JT, Pol A, Reimann J, Op Den Camp HJM. 2014. PQQ-dependent methanol dehydrogenases: Rare-earth elements make a difference. Appl Microbiol Biotechnol 98:6163-83.

28. Good NM, Vu HN, Suriano CJ, Subuyuj GA, Skovran E, Martinez-Gomez NC. 2016. Pyrroloquinoline Quinone-Containing Ethanol Dehydrogenase in *Methylobacterium extorquens* AM1 Extends Lanthanide-Dependent Metabolism to Multi-Carbon Substrates. J Bacteriol 198:3109–3118.

29. Schmidt S, Christen P, Kiefer P, Vorholt JA. 2010. Functional investigation of methanol dehydrogenase-like protein XoxF in *Methylobacterium extorquens* AM1. Microbiology 156:2575–86.

30. Hibi Y, Asai K, Arafuka H, Hamajima M, Iwama T, Kawai K. 2011. Molecular structure of La^{3+}-induced methanol dehydrogenase-like protein in *Methylobacterium radiotolerans*. J Biosci Bioeng 111:547–9.

31. Nakagawa T, Mitsui R, Tani A, Sasa K, Tashiro S, Iwama T, Hayakawa T, Kawai K. 2012. A catalytic role of XoxF1 as La^{3+}-dependent methanol dehydrogenase in *Methylobacterium extorquens* strain AM1. PLoS One 7:e50480.

32. Harms N, Ras J, Koning S, Reijnders WNM, Stouthamer AH, van Spanning RJM. 1996. Genetics of C1 metabolism regulation in *Paracoccus denitrificans*, p. 126–132. *In* Lidstrom, ME, Tabita, FR (eds.), Microbial Growth on C1 Compounds. Kluwer Academic Publishers, Dordrecht, The Netherlands.

33. Ramachandran A, Walsh DA. 2015. Investigation of XoxF methanol dehydrogenases reveals new methylotrophic bacteria in pelagic marine and freshwater ecosystems. FEMS Microbiol Ecol 91.

34. Martinez-Gomez NC, Vu HN, Skovran E. 2016. Lanthanide Chemistry: From Coordination in Chemical Complexes Shaping Our Technology to Coordination in Enzymes Shaping Bacterial Metabolism. Inorg Chem 55:10083–10089.

35. Vu HN, Subuyuj GA, Vijayakumar S, Good NM, Martinez-Gomez NC, Skovran E. 2016. Lanthanide-dependent regulation of methanol oxidation systems in *Methylobacterium extorquens* AM1 and their contribution to methanol growth. J Bacteriol 198:1250–1259.

36. Klinger JM. 2015. A historical geography of rare earth elements: From discovery to the atomic age. Extr Ind Soc 2:572–580.

37. Bünzli J-CG. 2014. Review: Lanthanide coordination chemistry: from old concepts to coordination polymers. J Coord Chem 67:3706–3733.

38. Friedman HG, Choppin GR, Feuerbacher DG, Melorose J, Perroy R, Careas S. 1964. The Shapes of the f Orbitals. J Chem Educ 41:354–358.

39. Pitzer KS. 1979. Relativistic Effects on Chemical Properties. Acc Chem Res 12:272–276.

40. Rahm M, Hoffmann R, Ashcroft NW. 2016. Atomic and Ionic Radii of Elements 1-96. Chem - A Eur J 22:14625–14632.

41. Evans WJ. 2000. Perspectives in reductive lanthanide chemistry. Coord Chem Rev 207:263–283.

42. Depero LE, Arienti MT, Zocchi M. 1991. Structure and Properties of Lanthanide Catalysts : The Crystal and Molecular Structure of $SmBr_3$.4iPr(OH). Struct Chem 2:595–600.

43. Martin RB, Richardson FS. 1979. Lanthanides as probes for calcium in biological systems. Q Rev Biophys 2:181–209.

44. Harder S. 2010. From Limestone to Catalysis : Application of Calcium Compounds as Homogeneous Catalysts. Chem Rev 110:3852–3876.

45. Rahm M, Hoffmann R, Ashcroft NW. 2016. Atomic and Ionic Radii of Elements 1-96. Chem - A Eur J 22:14625–14632.

46. Hartwell LH, Hopfield JJ, Leibler S, Murray AW. 1999. From molecular to modular cell biology. Nature 402:47–52.

47. Ihmels J, Levy R, Barkai N. 2004. Principles of transcriptional control in the metabolic network of *Saccharomyces cerevisiae*. Nat Biotechnol 22:86–92.

48. Kreimer A, Borenstein E, Gophna U, Ruppin E. 2008. The evolution of modularity in bacterial metabolic networks. Proc Natl Acad Sci 105:6976–6981.

49. Leopoldini M, Russo N, Toscano M. 2007. The Preferred Reaction Path for the Oxidation of Methanol by PQQ-Containing Methanol Dehydrogenase: Addition–Elimination versus Hydride-Transfer Mechanism. Chem - A Eur J 13:2109–2117.

50. Chistoserdova L, Kalyuzhnaya MG, Lidstrom ME. 2009. The expanding world of methylotrophic metabolism. Annu Rev Microbiol 63:477–99.

51. Vorholt J a., Chistoserdova L, Lidstrom ME, Thauer RK. 1998. The NADP-dependent methylene tetrahydromethanopterin dehydrogenase in *Methylobacterium extorquens* AM1. J Bacteriol 180:5351–5356.

52. Pomper BK, Vorholt JA, Chistoserdova L, Lidstrom ME, Thauer RK. 1999. A methenyl tetrahydromethanopterin cyclohydrolase and a methenyl tetrahydrofolate cyclohydrolase in *Methylobacterium extorquens* AM1. Eur J Biochem 261:475–480.

53. Chistoserdova L, Vorholt JA, Thauer RK, Lidstrom ME. 1998. C1 transfer enzymes and coenzymes linking methylotrophic bacteria and methanogenic Archaea. Science 281:99–102.

54. Maia LB, Moura JJG, Moura I. 2015. Molybdenum and tungsten-dependent formate dehydrogenases. J Biol Inorg Chem. Springer Berlin Heidelberg.

55. Chistoserdova L, Crowther GJ, Vorholt JA, Skovran E, Portais JCJ-C, Lidstrom ME. 2007. Identification of a Fourth Formate Dehydrogenase in *Methylobacterium extorquens* AM1 and Confirmation of the Essential Role of Formate Oxidation in Methylotrophy. J Bacteriol 189:9076–9081.

56. Laukel M, Chistoserdova L, Lidstrom ME, Vorholt J a. 2003. The tungsten-containing

formate dehydrogenase from *Methylobacterium extorquens* AM1: Purification and properties. Eur J Biochem 270:325–333.

57. Chistoserdova L, Laukel M, Portais JC, Vorholt JA, Lidstrom ME. 2004. Multiple Formate Dehydrogenase Enzymes in the Facultative Methylotroph *Methylobacterium extorquens* AM1 Are Dispensable for Growth on Methanol. J Bacteriol 186:22–28.

58. Šmejkalová H, Erb TJ, Fuchs G, Smejkalová H, Erb TJ, Fuchs G. 2010. Methanol assimilation in *Methylobacterium extorquens* AM1: demonstration of all enzymes and their regulation. PLoS One 5.

59. Ghosh M, Anthony C, Harlos K, Goodwin MG, Blake C. 1995. The refined structure of the quinoprotein methanol dehydrogenase from *Methylobacterium extorquens* at 1.94 Å. Structure 3:177–87.

60. Peyraud R, Schneider K, Kiefer P, Massou S, Vorholt J a, Portais J-C. 2011. Genome-scale reconstruction and system level investigation of the metabolic network of *Methylobacterium extorquens* AM1. BMC Syst Biol 5:189.

61. Schneider K, Peyraud R, Kiefer P, Christen P, Delmotte N, Massou S, Portais JC, Vorholt J a. 2012. The ethylmalonyl-CoA pathway is used in place of the glyoxylate cycle by *Methylobacterium extorquens* AM1 during growth on acetate. J Biol Chem 287:757–766.

62. Nunn DN, Lidstrom ME. 1986. Isolation and complementation analysis of 10 methanol oxidation mutant classes and identification of the methanol dehydrogenase structural gene of *Methylobacterium sp.* strain AM1. J Bacteriol 166:581–90.

63. Delaney NF, Kaczmarek ME, Ward LM, Swanson PK, Lee M-C, Marx CJ. 2013. Development of an optimized medium, strain and high-throughput culturing methods for *Methylobacterium extorquens*. PLoS One 8:e62957.

64. Strovas TJ, Sauter LM, Guo X, Lidstrom ME. 2007. Cell-to-cell heterogeneity in growth rate and gene expression in *Methylobacterium extorquens* AM1. J Bacteriol 189:7127–33.

65. Guo X, Lidstrom ME. 2006. Physiological analysis of *Methylobacterium extorquens* AM1 grown in continuous and batch cultures. Arch Microbiol 186:139–49.

66. Johnson BK, Scholz MB, Teal TK, Abramovitch RB. 2016. SPARTA: Simple Program for Automated reference-based bacterial RNA-seq Transcriptome Analysis. BMC Bioinformatics 17:66.

67. Quesenberry MS, Lee YC. 1996. A rapid formaldehyde assay using purpald reagent: application under periodation conditions. Anal Biochem 234:50–5.

68. Carroll SM, Marx CJ. 2013. Evolution after Introduction of a Novel Metabolic Pathway Consistently Leads to Restoration of Wild-Type Physiology. PLoS Genet 9:e1003427.

69. Gotoh K, Nakajima Y, Tajima G, Hotta Y, Kataoka T, Kawade Y, Sugiyama N, Ito T, Kimura K, Maeda Y. 2015. Assay for methylmalonyl coenzyme A mutase activity based on determination of succinyl coenzyme A by ultrahigh-performance liquid

chromatography tandem mass spectrometry. New Applications of Mass Spectrometry in Biomedicine. Anal Bioanal Chem 407:5281–5286.

70. Karr DB, Waters JK, Emerich DW. 1983. Analysis of Poly-3-Hydroxybutyrate in *Rhizobium japonicum* Bacteroids by Ion-Exclusion High-Pressure Liquid Chromatography and UV Detection. Appplied and Environmental Microbiology. 46:1339–1344.

71. Skovran E, Palmer AD, Rountree AM, Good NM, Lidstrom ME. 2011. XoxF is required for expression of methanol dehydrogenase in *Methylobacterium extorquens* AM1. J Bacteriol 193:6032–6038.

72. Martinez-Gomez NC, Good NM, Lidstrom ME. 2015. Methenyl-Dephosphotetrahydromethanopterin Is a Regulatory Signal for Acclimation to Changes in Substrate Availability in *Methylobacterium extorquens* AM1. J Bacteriol 197:2020–2026.

73. Heinrich D, Raberg M, Steinbuchel a., Steinbüchel A. 2015. Synthesis of poly(3-hydroxybutyrate-co-3-hydroxyvalerate) from unrelated carbon sources in engineered *Rhodospirillum rubrum*. FEMS Microbiol Lett 362:fnv038-fnv038.

74. Trainer MA, Charles TC. 2006. The role of PHB metabolism in the symbiosis of rhizobia with legumes. Appl Microbiol Biotechnol.